

**Theory and Software for Light Scattering
From Multilayer Optical Components
With Interfacial Roughness**

by
J. Merle Elson
Research Department

OCTOBER 1992

NAVAL AIR WARFARE CENTER WEAPONS DIVISION
CHINA LAKE, CA 93555-6001



Approved for public release; distribution is unlimited.

19941212 009

Naval Air Warfare Center Weapons Division

FOREWORD

This report documents a study conducted during fiscal year 1992 at the Naval Air Warfare Center Weapons Division, China Lake, California. Support was provided by the Office of Naval Research Independent Research funding. The work was performed to document both theory and software as tools to predict light scattering resulting from interface roughness of multilayer optical components.

This report has been reviewed for technical accuracy by J. L. Stanford.

Approved by
R. L. DERR, *Head*
Research Department
29 October 1992

Under authority of
W. E. NEWMAN
RAdm., U.S. Navy
Commander

Released for publication by
W. B. PORTER
Deputy Commander for Research & Development

NAWCWPNS Technical Publication 8084

Published by Technical Information Department
Collation Cover, 24 leaves
First printing 80 copies

REPORT DOCUMENTATION PAGE

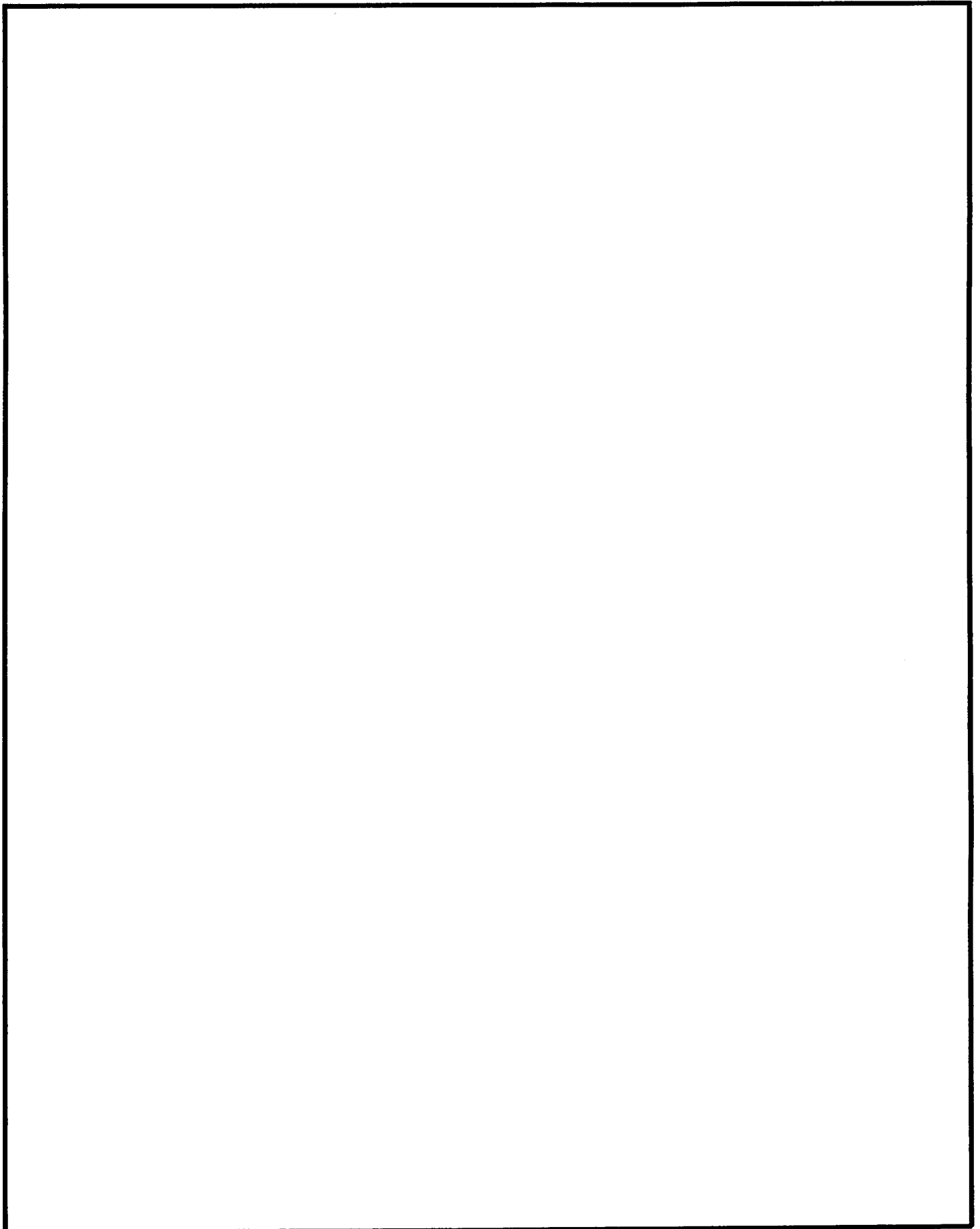
Form Approved
OMB No. 0704-0188

Public reporting burden for this collection of information is estimated to average 1 hour per response, including the time for reviewing instructions, searching existing data sources, gathering and maintaining the data needed, and completing and reviewing the collection of information. Send comments regarding this burden estimate or any other aspect of this collection of information, including suggestions for reducing this burden, to Washington Headquarters Services, Directorate for Information Operations and Reports, 1215 Jefferson Davis Highway, Suite 1204, Arlington, VA 22202-4302, and to the Office of Management and Budget, Paperwork Reduction Project (0704-0188), Washington, DC 20503.

1. AGENCY USE ONLY (Leave blank)		2. REPORT DATE October 1992	3. REPORT TYPE AND DATES COVERED Final Fiscal Year 1992	
4. TITLE AND SUBTITLE THEORY AND SOFTWARE FOR LIGHT SCATTERING FROM MULTILAYER OPTICAL COMPONENTS WITH INTERFACIAL ROUGHNESS			5. FUNDING NUMBERS N0001492WX4E012 PE 61152N R00N0	
6. AUTHOR(S) J. Merle Elson				
7. PERFORMING ORGANIZATION NAME(S) AND ADDRESS(ES) Naval Air Warfare Center Weapons Division China Lake, CA 93555-6001			8. PERFORMING ORGANIZATION REPORT NUMBER NAWCWPNS TP 8084	
9. SPONSORING/MONITORING AGENCY NAME(S) AND ADDRESS(ES) Office of Naval Research Arlington, VA 22217-5660			10. SPONSORING/MONITORING AGENCY REPORT NUMBER	
11. SUPPLEMENTARY NOTES				
12A. DISTRIBUTION/AVAILABILITY STATEMENT A Statement; public release; distribution unlimited			12B. DISTRIBUTION CODE	
13. ABSTRACT (Maximum 200 words) (U) First-order perturbation theory is applied to calculate the angular distribution of light scattered when a monochromatic plane wave illuminates a multilayer optical component. The light scattering is assumed to be caused by random roughness at each interface of the multilayer component where the root-mean-square (rms) roughness at any interface is assumed to be much less than the incident wavelength. Input parameters include the incident polarization, angle of incidence, wavelength, rms, and correlation length values for each interface, as well as the design of the multilayer stack. The superstrate medium can be any lossless transparent material. The layers of the multilayer stack and substrate media can be transparent or metallic. Output includes scattered power per unit solid angle normalized to the incident power. The scattered field is considered in both reflection- and transmission-scattering hemispheres. Also, the polarization of the scattered field is retained. Correlated and uncorrelated statistical models for the interface roughness are considered; however, partial correlation is discussed. Numerous equations in the theory are related to the FORTRAN code software listing. Instructions are given to use the software for numerical analysis. Four examples are given along with input data files, listing of numerical output, and plots of numerical output.				
14. SUBJECT TERMS Light Scattering Thin Films BRDF			15. NUMBER OF PAGES 46	
			16. PRICE CODE	
17. SECURITY CLASSIFICATION OF REPORT UNCLASSIFIED		18. SECURITY CLASSIFICATION OF THIS PAGE UNCLASSIFIED	19. SECURITY CLASSIFICATION OF ABSTRACT UNCLASSIFIED	
			20. LIMITATION OF ABSTRACT UL	

UNCLASSIFIED

SECURITY CLASSIFICATION OF THIS PAGE *(When Data Entered)*



SECURITY CLASSIFICATION OF THIS PAGE

UNCLASSIFIED

NAWCWPNS TP 8084

Accession For	
NTIS CRA&I	<input checked="" type="checkbox"/>
DTIC TAB	<input type="checkbox"/>
Unannounced	<input type="checkbox"/>
Justification	
By _____	
Distribution/	
Availability Codes	
Dist	Avail and/or Special
A-1	

CONTENTS

1. Introduction	3
2. Basic Theory	3
3. Zero-Order Field	7
4. First-Order (Scattered) Field	12
5. Angular Distribution of Scattered Light	16
6. Power Spectral Density Functions	18
7. Computer Program and Numerical Examples	22
8. References	26
Appendixes:	
A. Correspondence Between Symbols Used in the Computer Code and Theory	27
B. FORTRAN Listing of Multilayer Scattering Source Code	29
C. Input Data and Output Results for Reflection and Transmission ARS From a Multilayer Stack With 28 Layers	39
D. Input Data and Output Results for Reflection and Transmission ARS From an Uncoated Surface and Total Internal Reflection of the Incident Beam	41
E. Input Data and Output Results for Out-of-Plane ARS From a Five-Layer Stack Upon a Metallic Substrate	43
F. Input Data and Output Results for ARS From a Semi-Opaque Thin Metallic Film Including Surface Plasma Resonance	45

1. INTRODUCTION

This document discusses a first-order vector perturbation theory calculation for angle-resolved scattering (ARS) from multilayered optical components having random roughness at each interface of the composite stack. The theoretical basis of this work was first developed and presented many years ago (Reference 1). Comparison between theory and experiment yielded good results (Reference 2). Since then, technological devices involving specialized multilayer optical components having many tens or hundreds of layers have been conceived or fabricated that depend critically on very high levels of performance such as 99.99% reflection or transmission. This means that scattered light, which is on the order of 0.01% or more of the incident energy either in reflection or transmission, may limit or destroy intended performance. Thus, knowledge of expected scattering characteristics for multilayer components in optical systems definitely can be a valuable design tool. This theory can be applied also to uncoated components.

Also, a Fortran source code for numerical evaluation of the theory presented here is given along with user instructions and sample output data. Formulas for reflection and transmission scattering are given and are related to the source code.

2. BASIC THEORY

The multilayer stack is assumed to be illuminated by a monochromatic plane wave of wavelength λ incident at polar angle θ_0 relative to the direction normal to the mean surface. Regarding polarization of the incident beam, the electric vector can be oriented at an arbitrary angle relative to the plane of incidence. Referring to Figure 1, interface j of the multilayer stack is described by $z = d_j + \Delta z_j(\vec{\rho})$, where $\Delta z_j(\vec{\rho})$ is a random variable that describes the surface roughness of interface j and fluctuates about the mean surface level d_j . The roughness of the interface j has a mean square value of $\langle |\Delta z_j(\vec{\rho})|^2 \rangle = \delta_j^2$ when averaged over the interface j , and $\vec{\rho} = (x, y)$ is a point on the mean surface reference plane of interface j . Since the

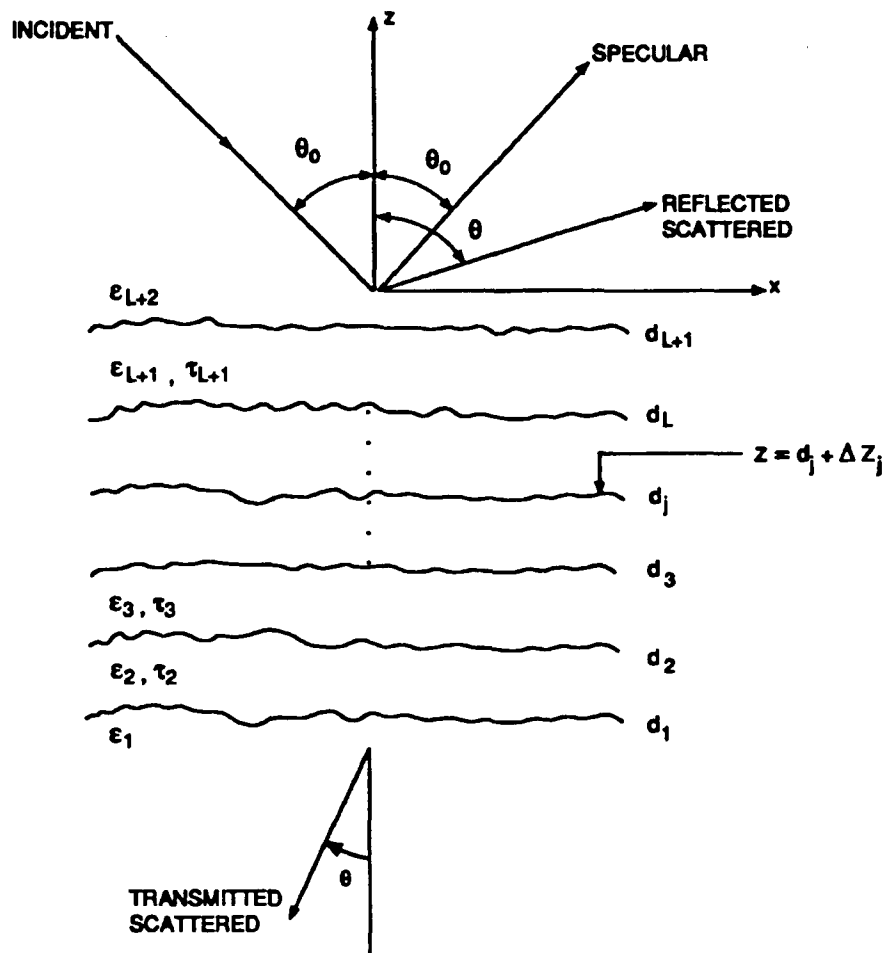


FIGURE 1. Schematic Showing Nomenclature Associated With the Multilayer System That Consists of a Substrate, L Layers, and a Superstrate. The superstrate contains the incident beam specular beam, and reflected scattered field. As shown, the substrate contains only the transmitted scattered field, if any, although there may also be a transmitted specular beam. The angles θ_0 and θ are the polar angle of incidence and scattering, respectively. The incident beam is assumed to be in the (x, z) plane. The scattered field has direction (θ, ϕ) where the azimuth angle ϕ is not shown here. The regions of the multilayer system have complex dielectric constants ϵ_j , where $j = 1$ is the substrate, $j = 2 \rightarrow L + 1$ are the layers of the stack with mean physical thicknesses τ_j , and $j = L + 2$ is the superstrate. The d_j are the cumulative thickness of the multilayer stack at the mean surface level of interface j , and the function $\Delta z_j(x, y)$ is the random roughness function, which deviates about $z = d_j$.

results given in this work are based on a first-order perturbation calculation, it is assumed that the ratio of root-mean-square (rms) roughness to wavelength δ_j/λ is much less than unity.

The multilayer stack has L layers, which are labeled $j = 2 \rightarrow L + 1$. The total multilayer system is assumed to consist of these L layers, each having physical thickness τ_j plus a semi-infinite substrate and superstrate. For convenience we will apply the term "layer" to the substrate and superstrate, where the substrate is layer $j = 1$ and the superstrate is layer $j = L + 2$. Thus, the total multilayer system has $L + 2$ layers. The homogeneous complex dielectric constant of layer j is ϵ_j , where $j = 1 \rightarrow L + 2$. In this work, the real part of ϵ_j can be positive or negative, but the imaginary part of ϵ_j is always positive.

In each layer of the multilayer system, we seek electric and magnetic field vector solutions of the wave equation having tangential components that are continuous to first-order in δ_j/λ across the rough interface j . As will be seen, this is equivalent to a distribution of surface currents at the planar mean interface. For interface j , the unit normal to first-order in δ_j/λ may be written

$$\hat{n}_j = \hat{z} - \hat{x} \left(\frac{\partial \Delta z_j(\vec{\rho})}{\partial x} \right) - \hat{y} \left(\frac{\partial \Delta z_j(\vec{\rho})}{\partial y} \right) \quad (2.1)$$

In order to satisfy the conditions of continuity, the electric field in medium j may be written as a sum of zero- and first-order fields, $\vec{E}_j(\vec{\rho}, z) = \vec{E}_j^{(0)}(\vec{\rho}, z) + \vec{E}_j^{(1)}(\vec{\rho}, z)$. This may be expanded to first-order about the $z = d_j$ plane to approximate the electric field at $z = d_j + \Delta z(\vec{\rho})$, and this yields

$$\vec{E}_j(\vec{\rho}, d_j + \Delta z(\vec{\rho})) = \vec{E}_j^{(0)}(\vec{\rho}, d_j) + \Delta z_j(\vec{\rho}) \frac{\partial \vec{E}_j^{(0)}(\vec{\rho}, z)}{\partial z} \Big|_{z=d_j} + \vec{E}_j^{(1)}(\vec{\rho}, d_j) \quad (2.2)$$

The $\vec{E}_j^{(0)}$ is the zero-order field solution for layer j that results when all interfaces are perfectly smooth, i. e., $\Delta z_j(\vec{\rho}) = 0$ for all j . The $\vec{E}_j^{(1)}$ is the first-order correction (scattered field) to the total electric field for layer j , which arises as a result of interface roughness. Considering first the boundary condition that the tangential components of the electric field given in Equation 2.2 be continuous across interfaces j and $j + 1$, we have

$$\hat{n} \times \Delta \vec{E}_{j+1,j}(\vec{\rho}, d_j + \Delta z_j(\vec{\rho})) = 0 \quad (2.3)$$

where

$$\Delta \vec{E}_{j+1,j}(\vec{\rho}, d_j + \Delta z_j(\vec{\rho})) = \vec{E}_{j+1}(\vec{\rho}, d_j + \Delta z_j(\vec{\rho})) - \vec{E}_j(\vec{\rho}, d_j + \Delta z_j(\vec{\rho})) \quad (2.4)$$

is the difference of the electric fields evaluated across the $z = d_j + \Delta z_j(\vec{\rho})$ boundary. Using Equations 2.1 and 2.2 in Equation 2.3 yields

$$\Delta E_{j+1,j,x}^{(1)}(\vec{\rho}, \Delta z_j(\vec{\rho})) = - \left(\frac{\partial}{\partial x} \Delta z_j(\vec{\rho}) \right) \Delta E_{j+1,j,x}^{(0)}(\vec{\rho}, d_j) - \Delta z_j(\vec{\rho}) \Delta \left(\frac{\partial}{\partial z} E_{j+1,j,x}^{(0)}(\vec{\rho}, z) \right)_{z=d_j} \quad (2.5a)$$

and

$$\Delta E_{j+1,j,y}^{(1)}(\vec{\rho}, \Delta z_j(\vec{\rho})) = - \left(\frac{\partial}{\partial y} \Delta z_j(\vec{\rho}) \right) \Delta E_{j+1,j,y}^{(0)}(\vec{\rho}, d_j) - \Delta z_j(\vec{\rho}) \Delta \left(\frac{\partial}{\partial z} E_{j+1,j,y}^{(0)}(\vec{\rho}, z) \right)_{z=d_j} \quad (2.5b)$$

for discontinuities of the x- and y-components of $\vec{E}_j^{(1)}$ and $\vec{E}_{j+1}^{(1)}$ across interface j .

We assume that the zero-order field in layer j has the form

$$\vec{E}_j^{(0)}(\vec{\rho}, z) = \vec{e}_j^{(0)}(\vec{k}_0, z) e^{i\vec{k}_0 \cdot \vec{\rho}} = \vec{e}_j^{(0)}(k_0, z) e^{ik_0 x} \quad (2.6a)$$

which indicates that the incident beam is in the (x, z) plane where the vector $\vec{k}_0 = \hat{x}k_0 = \hat{x}(\omega/c)\sqrt{\epsilon_{L+2}} \sin \theta_0$ is the projection of the incident wave vector onto the mean surface plane. Note that the incident medium ($j = L + 2$) must be lossless.

The first-order field in layer j is written as a Fourier integral

$$\vec{E}_j^{(1)}(\vec{\rho}, z) = \left(\frac{1}{2\pi} \right)^2 \int d^2 k \vec{e}_j^{(1)}(\vec{k}, z) e^{i\vec{k} \cdot \vec{\rho}} \quad (2.6b)$$

where $\vec{k} = (k_x, k_y)$ is the projection of the scattered field wave vector on the (x, y) plane. An $\exp(-i\omega t)$ time dependence is assumed but not shown explicitly. Using Equations 2.6 in Equations 2.5 yields

$$(2\pi)^2 \Delta e_{j+1,j,x}^{(1)}(\vec{k}, d_j) = -ik_x \Delta e_{j+1,j,x}^{(0)}(k_0, d_j) \Delta z_j(\vec{k}_0 - \vec{k}) \quad (2.7a)$$

and

$$(2\pi)^2 \Delta e_{j+1,j,y}^{(1)}(\vec{k}, d_j) = -ik_y \Delta e_{j+1,j,z}^{(0)}(k_0, d_j) \Delta Z_j(\vec{k}_0 - \vec{k}) \quad (2.7b)$$

where

$$\Delta Z_j(\vec{k}_0 - \vec{k}) = \int d^2 \rho \Delta z_j(\vec{\rho}) e^{i(\vec{k}_0 - \vec{k}) \cdot \vec{\rho}} \quad (2.8)$$

These equations indicate that the x - and y -components of the first-order electric field solution are discontinuous across the mean planar surface at $z = d_j$. This implies that there is a sheet of Dirac δ -function surface currents at the plane $z = d_j$ that is equivalent to the roughness (Reference 3). Equation 2.8 is the Fourier transform of the profile for interface j .

Similar continuity equations for the x - and y -components of the magnetic field yield

$$(2\pi)^2 \Delta h_{j+1,j,x}^{(1)}(\vec{k}, d_j) = i(\omega/c) \Delta d_{j+1,j,y}^{(0)}(k_0, d_j) \Delta Z_j(\vec{k}_0 - \vec{k}) \quad (2.9a)$$

and

$$(2\pi)^2 \Delta h_{j+1,j,y}^{(1)}(\vec{k}, d_j) = -i(\omega/c) \Delta d_{j+1,j,x}^{(0)}(k_0, d_j) \Delta Z_j(\vec{k}_0 - \vec{k}) \quad (2.9b)$$

where the displacement vector $\vec{D}_j^{(0)} = \epsilon_j \vec{E}_j^{(0)}$ and

$$\Delta \vec{d}_{j+1,j}^{(0)}(k_0, d_j) = [\epsilon_{j+1} \vec{e}_{j+1}^{(0)}(k_0, d_j) - \epsilon_j \vec{e}_j^{(0)}(k_0, d_j)] \quad (2.10)$$

The first-order scattered field is obtained primarily by finding solutions to Maxwell's equations that have discontinuities as given in Equations 2.7 and 2.9. This requires solution of the zero-order field.

3. ZERO-ORDER FIELD

The wave equation for the zero-order electric field in layer j of the multilayer system is written as

$$[\nabla^2 + (\omega/c)^2 \epsilon_j] \vec{E}_j^{(0)}(\vec{\rho}, z) = 0 \quad (3.1)$$

Assume layer $L + 1$ is illuminated by a linearly polarized plane wave with wave vector in

the x - z plane incident at polar angle θ_0 relative to the z -axis. The incident beam may be written as the sum of a p-polarized (electric vector parallel to plane of incidence) and s-polarized (electric vector perpendicular to plane of incidence) component. Thus, the zero-order electric field amplitude solution to Maxwell's equations for layer j has the general form

$$\vec{E}_j^{(0)}(\vec{\rho}, z) = \vec{E}_{j,p}^{(0)}(\vec{\rho}, z) + \vec{E}_{j,s}^{(0)}(\vec{\rho}, z) \quad (3.2)$$

where the p- and s-polarized component solutions are

$$\begin{aligned} \vec{E}_{j,p}^{(0)}(\vec{\rho}, z) &= \{\hat{x}e_{j,x}^{(0)}(z) + \hat{z}e_{j,z}^{(0)}(z)\} e^{ik_0x} \\ &= \cos\psi \left\{ a_j^{(0)} \frac{(\hat{x}q_j^{(0)} - \hat{z}k_0)}{(\omega/c)\sqrt{\epsilon_j}} e^{iq_j^{(0)}z} + b_j^{(0)} \frac{(\hat{x}q_j^{(0)} + \hat{z}k_0)}{(\omega/c)\sqrt{\epsilon_j}} e^{-iq_j^{(0)}z} \right\} e^{ik_0x} \end{aligned} \quad (3.3a)$$

and

$$\vec{E}_{j,s}^{(0)}(\vec{\rho}, z) = -\hat{y}e_{j,y}^{(0)}(z)e^{ik_0x} = -\hat{y} \sin\psi \left\{ g_j^{(0)} e^{iq_j^{(0)}z} + f_j^{(0)} e^{-iq_j^{(0)}z} \right\} e^{ik_0x} \quad (3.3b)$$

respectively. The angle of the electric vector relative to the plane of incidence is ψ . Thus, $\psi = 0$ degrees is p-polarized incidence and $\psi = 90$ degrees is s-polarized incidence. In layer j , we have $(\omega/c)^2\epsilon_j = k_0^2 + q_j^{(0)}$ or

$$q_j^{(0)} = [(\omega/c)^2\epsilon_j - k_0^2]^{1/2} \quad (3.4)$$

with $\omega/c = 2\pi/\lambda$. To compute the unknown coefficients $a_j^{(0)}$, $b_j^{(0)}$, $g_j^{(0)}$, and $f_j^{(0)}$, we equate tangential components of the electric and magnetic field amplitudes across the interface boundaries, use the facts that there are no incoming beams from the substrate region and that the incident intensity is of unit magnitude. This yields solutions of the form

$$a_j^{(0)} = -\frac{q_{L+2}^{(0)}P_{0,12}^{(1,j-1)}}{q_j^{(0)}P_{0,11}^{(1,L+1)}} \quad (3.5a)$$

$$b_j^{(0)} = \frac{q_{L+2}^{(0)}P_{0,11}^{(1,j-1)}}{q_j^{(0)}P_{0,11}^{(1,L+1)}} \quad (3.5b)$$

$$g_j^{(0)} = -\frac{q_{L+2}^{(0)} S_{0,12}^{(1,j-1)}}{q_j^{(0)} S_{0,11}^{(1,L+1)}} \quad (3.5c)$$

$$f_j^{(0)} = \frac{q_{L+2}^{(0)} S_{0,11}^{(1,j-1)}}{q_j^{(0)} S_{0,11}^{(1,L+1)}} \quad (3.5d)$$

where $j = 1 \rightarrow L + 2$.

For $j = 2 \rightarrow L + 2$, the matrix elements $P_{0,11}^{(1,j-1)}$ and $P_{0,12}^{(1,j-1)}$ are derived from the matrix product

$$P_0^{(1,j-1)} = \begin{pmatrix} P_{0,11}^{(1,j-1)} & P_{0,12}^{(1,j-1)} \\ P_{0,21}^{(1,j-1)} & P_{0,22}^{(1,j-1)} \end{pmatrix} = P_0^{(1)} P_0^{(2)} \dots P_0^{(j-1)} \quad (3.6a)$$

and when $j = 1$, we define

$$P_0^{(1,0)} = \begin{pmatrix} P_{0,11}^{(1,0)} & P_{0,12}^{(1,0)} \\ P_{0,21}^{(1,0)} & P_{0,22}^{(1,0)} \end{pmatrix} = \begin{pmatrix} 1 & 0 \\ 0 & 1 \end{pmatrix} \quad (3.6b)$$

For $m = 1 \rightarrow L + 1$, the 2×2 matrices in the product on the far right of Equation 3.6a have the form

$$P_0^{(m)} = \begin{pmatrix} P_{0,11}^{(m)} & P_{0,12}^{(m)} \\ P_{0,21}^{(m)} & P_{0,22}^{(m)} \end{pmatrix} \quad (3.7a)$$

where the elements are given by

$$P_{0,11}^{(m)} = \left(\frac{\epsilon_m q_{m+1}^{(0)} + \epsilon_{m+1} q_m^{(0)}}{2q_m^{(0)} \sqrt{\epsilon_m \epsilon_{m+1}}} \right) \exp[i(q_{m+1}^{(0)} - q_m^{(0)})d_m] \quad (3.7b)$$

$$P_{0,12}^{(m)} = \left(\frac{\epsilon_m q_{m+1}^{(0)} - \epsilon_{m+1} q_m^{(0)}}{2q_m^{(0)} \sqrt{\epsilon_m \epsilon_{m+1}}} \right) \exp[-i(q_{m+1}^{(0)} + q_m^{(0)})d_m] \quad (3.7c)$$

$$p_{0,21}^{(m)} = \left(\frac{\epsilon_m q_{m+1}^{(0)} - \epsilon_{m+1} q_m^{(0)}}{2q_m^{(0)} \sqrt{\epsilon_m \epsilon_{m+1}}} \right) \exp[i(q_{m+1}^{(0)} + q_m^{(0)})d_m] \quad (3.7d)$$

$$p_{0,22}^{(m)} = \left(\frac{\epsilon_m q_{m+1}^{(0)} + \epsilon_{m+1} q_m^{(0)}}{2q_m^{(0)} \sqrt{\epsilon_m \epsilon_{m+1}}} \right) \exp[-i(q_{m+1}^{(0)} - q_m^{(0)})d_m] \quad (3.7e)$$

The corresponding s-polarized field matrix elements $S_{0,11}^{(1,j-1)}$ and $S_{0,12}^{(1,j-1)}$ for $j = 2 \rightarrow L + 2$ are given by the matrix product

$$S_0^{(1,j-1)} = \begin{pmatrix} S_{0,11}^{(1,j-1)} & S_{0,21}^{(1,j-1)} \\ S_{0,21}^{(1,j-1)} & S_{0,22}^{(1,j-1)} \end{pmatrix} = s_0^{(1)} s_0^{(2)} \dots s_0^{(j-1)} \quad (3.8a)$$

and for $j = 1$, we define

$$S_0^{(1,0)} = \begin{pmatrix} S_{0,11}^{(1,0)} & S_{0,12}^{(1,0)} \\ S_{0,21}^{(1,0)} & S_{0,22}^{(1,0)} \end{pmatrix} = \begin{pmatrix} 1 & 0 \\ 0 & 1 \end{pmatrix} \quad (3.8b)$$

For $m = 1 \rightarrow L + 1$, the 2×2 matrices in the product on the far right of Equation 3.8a have the form

$$s_0^{(m)} = \begin{pmatrix} s_{0,11}^{(m)} & s_{0,12}^{(m)} \\ s_{0,21}^{(m)} & s_{0,22}^{(m)} \end{pmatrix} \quad (3.9a)$$

where the elements are given by

$$s_{0,11}^{(m)} = \left(\frac{q_m^{(0)} + q_{m+1}^{(0)}}{2q_m^{(0)}} \right) \exp[i(q_{m+1}^{(0)} - q_m^{(0)})d_m] \quad (3.9b)$$

$$s_{0,12}^{(m)} = \left(\frac{q_m^{(0)} - q_{m+1}^{(0)}}{2q_m^{(0)}} \right) \exp[-i(q_{m+1}^{(0)} + q_m^{(0)})d_m] \quad (3.9c)$$

$$s_{0,21}^{(m)} = \left(\frac{q_m^{(0)} - q_{m+1}^{(0)}}{2q_m^{(0)}} \right) \exp[i(q_{m+1}^{(0)} + q_m^{(0)})d_m] \quad (3.9d)$$

$$s_{0,22}^{(m)} = \left(\frac{q_m^{(0)} + q_{m+1}^{(0)}}{2q_m^{(0)}} \right) \exp[-i(q_{m+1}^{(0)} - q_m^{(0)})d_m] \quad (3.9e)$$

In Equations 3.5 for $j = L + 2$, the $b_{L+2}^{(0)} = f_{L+2}^{(0)} = 1$, which validates the assumption that with Equations 3.3 the amplitude coefficient for the incident beam in the superstrate is of unit magnitude. Further, with Equations 3.5, we see from Equations 3.6b and 3.8b that $a_1^{(1,0)} = g_1^{(1,0)} = 0$ which validates the assumption that there are no incident beams from the substrate medium.

At this point, the zero-order field is solved and the intensity reflection R and transmission T for a p- or s-polarized incident beam are given by

$$R_p = |a_{L+2}^{(0)}|^2 \quad (3.10a)$$

$$T_p = |b_1^{(0)}|^2 \Re(q_1^{(0)})/\Re(q_{L+2}^{(0)}) \quad (3.10b)$$

$$R_s = |g_{L+2}^{(0)}|^2 \quad (3.10c)$$

$$T_s = |f_1^{(0)}|^2 \Re(q_1^{(0)})/\Re(q_{L+2}^{(0)}) \quad (3.10d)$$

where $\Re(Q)$ denotes the real part of Q .

The average flow of power from the superstrate region incident upon the $j = L + 1$ interface may be calculated from

$$P_0 = \frac{c}{8\pi} \Re \int_A d^2\rho (\overline{E}_{L+2}^{(0)} \times \overline{H}_{L+2}^{(0)}) \cdot \hat{z} = \frac{c}{8\pi} A \Re[q_{L+2}^{(0)}/(\omega/c)] \quad (3.11)$$

where only the incoming parts of $\overline{E}_{L+2}^{(0)}$ and $\overline{H}_{L+2}^{(0)}$ are retained, i. e., those terms proportional to $b_{L+2}^{(0)}$ and $f_{L+2}^{(0)}$ in Equations 3.3. The integration is over the area A of illumination, which has dimensions assumed to be essentially infinite compared to wavelength λ . It is further assumed in this work that the dielectric constant ϵ_{L+2} of the incident medium is nonabsorbing, and thus $q_{L+2}^{(0)}$ is also real.

4. FIRST-ORDER (SCATTERED) FIELD

Breaking Equation 2.6b into p- and s-polarization components, the first-order solution for the scattered electric field in layer j is rewritten:

$$\vec{E}_j^{(1)}(\vec{\rho}, z) = \left(\frac{1}{2\pi} \right)^2 \int d^2k \{ \vec{e}_{j,p}^{(1)}(z) + \vec{e}_{j,s}^{(1)}(z) \} e^{i\vec{k} \cdot \vec{\rho}} \quad (4.1a)$$

and the magnetic field is obtained from

$$\vec{H}_j^{(1)}(\vec{\rho}, z) = \frac{\vec{\nabla} \times \vec{E}_j^{(1)}(\vec{\rho}, z)}{i(\omega/c)} \quad (4.1b)$$

where

$$\vec{e}_{j,p}^{(1)}(z) = a_j^{(1)} \frac{(\vec{k}q_j^{(1)} - \hat{z}k)}{(\omega/c)\sqrt{\epsilon_j}} e^{iq_j^{(1)}z} + b_j^{(1)} \frac{(\vec{k}q_j^{(1)} + \hat{z}k)}{(\omega/c)\sqrt{\epsilon_j}} e^{-iq_j^{(1)}z} \quad (4.1c)$$

and

$$\vec{e}_{j,s}^{(1)}(z) = (\hat{k} \times \hat{z}) \{ g_j^{(1)} e^{iq_j^{(1)}z} + f_j^{(1)} e^{-iq_j^{(1)}z} \} \quad (4.1d)$$

The in-surface wave vector of the scattered field is

$$\vec{k} = \hat{k}k = (\hat{x} \cos \phi + \hat{y} \sin \phi)k = (k_x, k_y) \quad (4.2a)$$

where ϕ is the azimuth angle of scattering relative to the \hat{x} direction. Since we require $(\omega/c)^2 \epsilon_j = k^2 + q_j^{(1)2}$, the magnitude of the z-component of the scattered field wave vector is

$$q_j^{(1)} = [(\omega/c)^2 \epsilon_j - k^2]^{1/2} \quad (4.2b)$$

The k is generally different for scattering into different media. This is discussed further in the following section. In this work, we only calculate scattering into the reflection (ϵ_{L+2} medium) and transmission (ϵ_1 medium) hemispheres rather than into any of the L layers between these two semi-infinite media.

The coefficients $a_{L+2}^{(1)}$ and $g_{L+2}^{(1)}$ are called the reflection scattering coefficients. The $b_1^{(1)}$ and $f_1^{(1)}$ are the transmission scattering coefficients. These coefficients are calculated by application of Equations 2.7 and 2.9 with Equations 4.1 and can be written after some manipulation as a sum over the $L + 1$ interfaces as

$$a_{L+2}^{(1)} = \frac{1}{2P_{1,11}^{(1,L+1)}} \sum_{j=1}^{L+1} \Delta Z_j(\vec{k}_0 - \vec{k}) \left\{ \frac{(\omega/c)\sqrt{\epsilon_j}}{q_j^{(1)}} Y_{1,j}^{(0)} \eta_1^{(1,j-1)} - \frac{1}{\sqrt{\epsilon_j}} Y_{2,j}^{(0)} \eta_2^{(1,j-1)} \right\} \quad (4.3a)$$

$$g_{L+2}^{(1)} = -\frac{(\omega/c)}{2S_{1,11}^{(1,L+1)}} \sum_{j=1}^{L+1} \frac{\Delta Z_j(\vec{k}_0 - \vec{k})}{q_j^{(1)}} X_j^{(0)} \xi_1^{(1,j-1)} \quad (4.3b)$$

$$b_1^{(1)} = -\frac{1}{2P_{1,11}^{(1,L+1)}} \sum_{j=1}^{L+1} \Delta Z_j(\vec{k}_0 - \vec{k}) \left\{ \frac{(\omega/c)\sqrt{\epsilon_j}}{q_j^{(1)}} Y_{1,j}^{(0)} \mu_1^{(1,j-1)} - \frac{1}{\sqrt{\epsilon_j}} Y_{2,j}^{(0)} \mu_2^{(1,j-1)} \right\} \quad (4.4a)$$

$$f_1^{(1)} = \frac{(\omega/c)}{2S_{1,11}^{(1,L+1)}} \sum_{j=1}^{L+1} \frac{\Delta Z_j(\vec{k}_0 - \vec{k})}{q_j^{(1)}} X_j^{(0)} \{S_{11}^{(1,L+1)} \xi_2^{(1,j-1)} - S_{21}^{(1,L+1)} \xi_1^{(1,j-1)}\} \quad (4.4b)$$

The $\Delta Z_j(\vec{k}_0 - \vec{k})$ is the Fourier transform of the interface roughness function $\Delta z_j(\vec{\rho})$ as given in Equation 2.8. The $X_j^{(0)}$, $Y_{1,j}^{(0)}$, and $Y_{2,j}^{(0)}$ are called the zero-order source terms and may be written as

$$X_j^{(0)} = i(\omega/c) (\epsilon_{j+1} - \epsilon_j) \{e_{j,x}^{(0)}(d_j) \sin \phi - e_{j,y}^{(0)}(d_j) \cos \phi\} \quad (4.5a)$$

$$Y_{1,j}^{(0)} = ik \left(\frac{\epsilon_{j+1} - \epsilon_j}{\epsilon_{j+1}} \right) e_{j,z}^{(0)}(d_j) \quad (4.5b)$$

and

$$Y_{2,j}^{(0)} = i(\omega/c) (\epsilon_{j+1} - \epsilon_j) \{e_{j,x}^{(0)}(d_j) \cos \phi + e_{j,y}^{(0)}(d_j) \sin \phi\} \quad (4.5c)$$

To evaluate further the scattering coefficients in Equations 4.4, the ξ , η , and μ functions are required and these are defined by

$$\xi_1^{(1,j-1)} = S_{1,11}^{(1,j-1)} e^{-iq_j^{(1)} d_j} - S_{1,12}^{(1,j-1)} e^{iq_j^{(1)} d_j} \quad (4.6a)$$

$$\xi_{22}^{(1,j-1)} = S_{1,21}^{(1,j-1)} e^{-iq_j^{(1)} d_j} - S_{1,22}^{(1,j-1)} e^{iq_j^{(1)} d_j} \quad (4.6b)$$

$$\eta_1^{(1,j-1)} = P_{1,11}^{(1,j-1)} e^{-iq_j^{(1)} d_j} + P_{1,12}^{(1,j-1)} e^{iq_j^{(1)} d_j} \quad (4.7a)$$

$$\eta_2^{(1,j-1)} = P_{1,11}^{(1,j-1)} e^{-iq_j^{(1)} d_j} - P_{1,12}^{(1,j-1)} e^{iq_j^{(1)} d_j} \quad (4.7b)$$

$$\eta_3^{(1,j-1)} = P_{1,21}^{(1,j-1)} e^{-iq_j^{(1)} d_j} + P_{1,22}^{(1,j-1)} e^{iq_j^{(1)} d_j} \quad (4.7c)$$

$$\eta_4^{(1,j-1)} = P_{1,21}^{(1,j-1)} e^{-iq_j^{(1)} d_j} - P_{1,22}^{(1,j-1)} e^{iq_j^{(1)} d_j} \quad (4.7d)$$

$$\mu_1^{(1,j-1)} = P_{1,11}^{(1,L+1)} \eta_3^{(1,j-1)} - P_{1,21}^{(1,L+1)} \eta_1^{(1,j-1)} \quad (4.8a)$$

$$\mu_2^{(1,j-1)} = P_{1,11}^{(1,L+1)} \eta_4^{(1,j-1)} - P_{1,21}^{(1,L+1)} \eta_2^{(1,j-1)} \quad (4.8b)$$

The η and μ functions pertain to the p-polarized scattered field and require evaluation of the matrix products

$$P_1^{(1,j-1)} = \begin{pmatrix} P_{1,11}^{(1,j-1)} & P_{1,12}^{(1,j-1)} \\ P_{1,21}^{(1,j-1)} & P_{1,22}^{(1,j-1)} \end{pmatrix} = P_1^{(1)} P_1^{(2)} \dots P_1^{(j-1)} \quad (4.9a)$$

where $j = 2 \rightarrow L + 2$. For $j = 1$, we define

$$P_1^{(1,0)} = \begin{pmatrix} P_{1,11}^{(1,0)} & P_{1,12}^{(1,0)} \\ P_{1,21}^{(1,0)} & P_{1,22}^{(1,0)} \end{pmatrix} = \begin{pmatrix} 1 & 0 \\ 0 & 1 \end{pmatrix} \quad (4.9b)$$

where the 2×2 matrices in the product on the far right of Equation 4.9a have elements

$$P_{1,11}^{(m)} = \left(\frac{\epsilon_m q_{m+1}^{(1)} + \epsilon_{m+1} q_m^{(1)}}{2q_m^{(1)} \sqrt{\epsilon_m \epsilon_{m+1}}} \right) \exp[i(q_{m+1}^{(1)} - q_m^{(1)})d_m] \quad (4.10a)$$

$$P_{1,12}^{(m)} = \left(\frac{\epsilon_m q_{m+1}^{(1)} - \epsilon_{m+1} q_m^{(1)}}{2q_m^{(1)} \sqrt{\epsilon_m \epsilon_{m+1}}} \right) \exp[-i(q_{m+1}^{(1)} + q_m^{(1)})d_m] \quad (4.10b)$$

$$P_{1,21}^{(m)} = \left(\frac{\epsilon_m q_{m+1}^{(1)} - \epsilon_{m+1} q_m^{(1)}}{2q_m^{(1)} \sqrt{\epsilon_m \epsilon_{m+1}}} \right) \exp[i(q_{m+1}^{(1)} + q_m^{(1)})d_m] \quad (4.10c)$$

$$P_{1,22}^{(m)} = \left(\frac{\epsilon_m q_{m+1}^{(1)} + \epsilon_{m+1} q_m^{(1)}}{2q_m^{(1)} \sqrt{\epsilon_m \epsilon_{m+1}}} \right) \exp[-i(q_{m+1}^{(1)} - q_m^{(1)})d_m] \quad (4.10d)$$

For the ξ functions, which pertain to the s-polarized field, the corresponding matrices for $j = 2 \rightarrow L + 2$ are given by

$$S_1^{(1,j-1)} = \begin{pmatrix} S_{1,11}^{(1,j-1)} & S_{1,12}^{(1,j-1)} \\ S_{1,21}^{(1,j-1)} & S_{1,22}^{(1,j-1)} \end{pmatrix} = s_1^{(1)} s_1^{(2)} \dots s_1^{(j-1)} \quad (4.11a)$$

For $j = 1$, we define

$$S_1^{(1,0)} = \begin{pmatrix} S_{1,11}^{(1,0)} & S_{1,12}^{(1,0)} \\ S_{1,21}^{(1,0)} & S_{1,22}^{(1,0)} \end{pmatrix} = \begin{pmatrix} 1 & 0 \\ 0 & 1 \end{pmatrix} \quad (4.11b)$$

where the elements of the matrices on the far right of Equation 4.11a are

$$s_{1,11}^{(m)} = \left(\frac{q_m^{(1)} + q_{m+1}^{(1)}}{2q_m^{(1)}} \right) \exp[i(q_{m+1}^{(1)} - q_m^{(1)})d_m] \quad (4.12a)$$

$$s_{1,12}^{(m)} = \left(\frac{q_m^{(1)} - q_{m+1}^{(1)}}{2q_m^{(1)}} \right) \exp[-i(q_{m+1}^{(1)} + q_m^{(1)})d_m] \quad (4.12b)$$

$$s_{1,21}^{(m)} = \left(\frac{q_m^{(1)} - q_{m+1}^{(1)}}{2q_m^{(1)}} \right) \exp[i(q_{m+1}^{(1)} + q_m^{(1)})d_m] \quad (4.12c)$$

$$s_{1,22}^{(m)} = \left(\frac{q_m^{(1)} + q_{m+1}^{(1)}}{2q_m^{(1)}} \right) \exp[-i(q_{m+1}^{(1)} - q_m^{(1)})d_m] \quad (4.12d)$$

These $S_1^{(1,j-1)}$ and $P_1^{(1,j-1)}$ matrices are analogous to those used in the evaluation of the zero-order field coefficients as in Section 3.

5. ANGULAR DISTRIBUTION OF SCATTERED LIGHT

We seek a ratio $dP/d\Omega$ of power dP scattered into direction (θ, ϕ) divided by solid angle $d\Omega = \sin\theta d\theta d\phi$. This ratio, normalized by the total power incident on the surface P_0 , is the ARS, $(1/P_0)(dP/d\Omega)$. This expression is related to the bidirectional reflectance distribution function (*BRDF*) by

$$ARS = BRDF \cos\theta = \frac{1}{P_0} \frac{dP}{d\Omega} \quad (5.1)$$

Calculation of the ARS is accomplished by considering an integral of the form

$$P_j = \frac{c}{8\pi} \Re \int_A d^2\rho (\vec{E}_j^{(1)} \times \vec{H}_j^{(1)}) \cdot \hat{z} \quad (5.2)$$

where $j = L + 2$ for reflectance scattering and $j = 1$ for transmission scattering. For $j = L + 2$ and $j = 1$, P_j is the time-averaged energy propagating away from the multilayer stack in the positive and negative \hat{z} direction, respectively. Using Equations 4.1 for $j = L + 2$ in Equation 5.2 yields, after some manipulation,

$$P_{L+2} = \left(\frac{c^2}{8\pi\omega} \right) \left(\frac{1}{2\pi} \right)^2 \int d^2k q_{L+2}^{(1)} \{ |a_{L+2}^{(1)}|^2 + |g_{L+2}^{(1)}|^2 \} e^{-2z\Im\{q_{L+2}^{(1)}\}} \quad (5.3a)$$

and likewise for $j = 1$ we obtain

$$P_1 = - \left(\frac{c^2}{8\pi\omega} \right) \left(\frac{1}{2\pi} \right)^2 \int d^2k q_1^{(1)} \{ |b_1^{(1)}|^2 + |f_1^{(1)}|^2 \} e^{2z\Im\{q_1^{(1)}\}} \quad (5.3b)$$

where the minus sign arises from the fact that for transmission scattering, the energy flow is in the $-\hat{z}$ direction. This work always assumes that the incident medium is lossless where $\Im\{\epsilon_{L+2}\} = 0$ where $\Im\{Q\}$ denotes the imaginary part of Q and $\Re\{\epsilon_{L+2}\} \geq 1$. Also, when transmission scattering is considered, the substrate medium is likewise assumed to be lossless with $\Im\{\epsilon_1\} = 0$ and $\Re\{\epsilon_1\} \geq 1$. In general, however, ϵ_1 is complex with unrestricted real and imaginary parts such that $\Re\{\epsilon_1\}$ can be greater than or less than zero and $\Im\{\epsilon_1\}$ is greater than zero. Equations 5.3 represent energy flow as an integral sum over all possible scattered wave vectors k . However, not all wave vectors contribute to scattering, since in Equation

5.3a there is no energy flow in the \hat{z} direction when $\Im\{q_{L+2}^{(1)}\} \neq 0$. Likewise, in Equation 5.3b, there is no energy flow in the $-\hat{z}$ direction when $\Im\{q_1^{(1)}\} \neq 0$. In considering reflection scattering, it follows that $\Im\{q_{L+2}^{(1)}\} = 0$ unless $k > (\omega/c)\sqrt{\epsilon_{L+2}}$. Similarly, for transmission scattering when $k > (\omega/c)\sqrt{\epsilon_1}$, we see that $\Im\{q_1^{(1)}\} \neq 0$. These wave vector values $k = |\vec{k}|$, which cause $\Im\{q_{L+2}^{(1)}\} \neq 0$ and/or $\Im\{q_1^{(1)}\} \neq 0$, correspond to evanescent scattered modes such as surface plasmons or guided waves that propagate parallel to the interfaces and thus do not carry energy away from the surface. In this work we are interested only in scattered fields that carry energy away from the multilayer stack, and this can be accomplished in an ad hoc fashion for Equation 5.3a (reflection scattering) if we let

$$k_x = (\omega/c)\sqrt{\epsilon_{L+2}} \sin \theta \cos \phi \quad (5.4a)$$

and

$$k_y = (\omega/c)\sqrt{\epsilon_{L+2}} \sin \theta \sin \phi \quad (5.4b)$$

from which it follows that $k = (\omega/c)\sqrt{\epsilon_{L+2}} \sin \theta$ and

$$d^2k = (\omega/c)^2 \epsilon_{L+2} \cos \theta \sin \theta d\theta d\phi = (\omega/c)^2 \epsilon_{L+2} \cos \theta d\Omega \quad (5.4c)$$

Similarly for Equation 5.3b (transmission scattering) we let

$$k_x = (\omega/c)\sqrt{\epsilon_1} \sin \theta \cos \phi \quad (5.5a)$$

and

$$k_y = (\omega/c)\sqrt{\epsilon_1} \sin \theta \sin \phi \quad (5.5b)$$

from which it follows that $k = (\omega/c)\sqrt{\epsilon_1} \sin \theta$ and

$$d^2k = (\omega/c)^2 \epsilon_1 \cos \theta \sin \theta d\theta d\phi = (\omega/c)^2 \epsilon_1 \cos \theta d\Omega \quad (5.5c)$$

It is not necessary to choose the k_x and k_y as given in Equations 5.4 and 5.5 in an ad hoc manner. These results also are obtained by integrating Equations 4.1 by the method of stationary phase and then proceeding with Equation 5.2.

From Equation 5.3a with Equations 5.4, we can show that the ARS result for scattering

into the reflection hemisphere (medium ϵ_{L+2}) into direction (θ, ϕ) is

$$\frac{1}{P_0} \left\langle \frac{dP_{L+1}}{d\Omega} \right\rangle = \frac{(\omega/c)^2 q_{L+2}^{(1)} \epsilon_{L+2} \cos \theta \left\{ \langle |a_{L+2}^{(1)}|^2 \rangle + \langle |g_{L+2}^{(1)}|^2 \rangle \right\}}{(2\pi)^2 q_{L+2}^{(0)} A} \quad (5.6a)$$

where the first and second terms in the $\{\dots\}$ are for p- and s-polarization, respectively, of the scattered field relative to the plane of scattering given by $(\hat{\mathbf{k}}, \hat{\mathbf{z}})$. The corresponding result for scattering into the transmission hemisphere (medium ϵ_1) is

$$\frac{1}{P_0} \left\langle \frac{dP_1}{d\Omega} \right\rangle = \frac{(\omega/c)^2 q_1^{(1)} \epsilon_1 \cos \theta \left\{ \langle |b_1^{(1)}|^2 \rangle + \langle |f_1^{(1)}|^2 \rangle \right\}}{(2\pi)^2 q_{L+2}^{(0)} A} \quad (5.6b)$$

The angle brackets $\langle \dots \rangle$ denote an ensemble average. The ensemble average is needed because the $a_{L+2}^{(1)}$, $b_1^{(1)}$, $f_1^{(1)}$, and $g_{L+2}^{(1)}$ depend on statistical properties of the roughness functions $\Delta z_j(\vec{\rho})$, which are treated as random variables for interfaces $j = l \rightarrow L + 1$. These statistical properties appear in the power spectral density of the interface roughness, and this is discussed in the following section.

6. POWER SPECTRAL DENSITY FUNCTIONS

Since the surface roughness function $\Delta z_j(\vec{\rho})$ for interface j can never be known deterministically, a statistical treatment is required to obtain an average or expected result for the ARS. In this work, we assume that the surface area $A \rightarrow \infty$ and the statistical process is stationary, ergodic, and isotropic. This means that statistical properties are independent of position and that an ensemble average and spatial average yield identical results independent of direction. The averaging acts on the scattering coefficients as shown in Equations 5.6, and these coefficients are rewritten here as

$$\langle |a_{L+2}^{(1)}|^2 \rangle = \sum_{n=1}^{L+1} \sum_{m=1}^{L+1} A_n A_m^* \langle \Delta Z_n(\vec{k}_0 - \vec{k}) \Delta Z_m^*(\vec{k}_0 - \vec{k}) \rangle \quad (6.1a)$$

$$\langle |g_{L+2}^{(1)}|^2 \rangle = \sum_{n=1}^{L+1} \sum_{m=1}^{L+1} G_n G_m^* \langle \Delta Z_n(\vec{k}_0 - \vec{k}) \Delta Z_m^*(\vec{k}_0 - \vec{k}) \rangle \quad (6.1b)$$

$$\langle |b_{L+2}^{(1)}|^2 \rangle = \sum_{n=1}^{L+1} \sum_{m=1}^{L+1} B_n B_m^* \langle \Delta Z_n(\vec{k}_0 - \vec{k}) \Delta Z_m^*(\vec{k}_0 - \vec{k}) \rangle \quad (6.1c)$$

$$\langle |f_{L+2}^{(1)}|^2 \rangle = \sum_{n=1}^{L+1} \sum_{m=1}^{L+1} F_n F_m^* \langle \Delta Z_n(\vec{k}_0 - \vec{k}) \Delta Z_m^*(\vec{k}_0 - \vec{k}) \rangle \quad (6.1d)$$

where * denotes complex conjugate. The A_j , G_j , B_j , and F_j are given by

$$A_j = \frac{1}{2P_{1,11}^{(1,L+1)}} \left\{ \frac{(\omega/c)\sqrt{\epsilon_j}}{q_j^{(1)}} Y_{1,j}^{(0)} \eta_{11}^{(1,j-1)} - \frac{1}{\sqrt{\epsilon_j}} Y_{2,j}^{(0)} \eta_{12}^{(1,j-1)} \right\} \quad (6.2a)$$

$$G_j = -\frac{(\omega/c)X_j^{(0)}\xi_{s1}^{(1,j-1)}}{2S_{1,11}^{(1,L+1)}q_j^{(1)}} \quad (6.2b)$$

$$B_j = -\frac{1}{2P_{1,11}^{(1,L+1)}} \left\{ \frac{(\omega/c)\sqrt{\epsilon_j}}{q_j^{(1)}} Y_{1,j}^{(0)} \mu_{11}^{(1,j-1)} - \frac{1}{\sqrt{\epsilon_j}} Y_{2,j}^{(0)} \mu_{12}^{(1,j-1)} \right\} \quad (6.2c)$$

$$F_j = \frac{(\omega/c)X_j^{(0)}}{2S_{1,11}^{(1,L+1)}q_j^{(1)}} \{ S_{11}^{(1,L+1)}\xi_{s2}^{(1,j-1)} - S_{21}^{(1,L+1)}\xi_{s1}^{(1,j-1)} \} \quad (6.2d)$$

and we define

$$g_{nm}(\vec{k}_0 - \vec{k}) = \frac{\langle \Delta Z_n(\vec{k}_0 - \vec{k}) \Delta Z_m^*(\vec{k}_0 - \vec{k}) \rangle}{A} \quad (6.3)$$

which is the average cross-power spectral density for the spatial frequencies of the roughness between interfaces n and m . This average is easily shown to be related to the roughness correlation function by using Equation 2.8 in Equation 6.3, which yields

$$\begin{aligned} g_{nm}(\vec{k}_0 - \vec{k}) &= \int d^2\beta e^{i(\vec{k}_0 - \vec{k}) \cdot \vec{\beta}} \left\{ \lim_{A \rightarrow -A} \frac{1}{A} \int d^2\rho \Delta z_n(\vec{\rho} + \vec{\beta}) \Delta z_m(\vec{\rho}) \right\} \\ &= \int d^2\beta e^{i(\vec{k}_0 - \vec{k}) \cdot \vec{\beta}} G_{nm}(\beta) \end{aligned} \quad (6.4)$$

where the correlation function

$$G_{nm}(\beta) = \langle \Delta z_n(\vec{\rho} + \vec{\beta}) \Delta z_m(\vec{\rho}) \rangle = \lim_{A \rightarrow \infty} \left\{ \frac{1}{A} \int d^2\rho \Delta z_n(\vec{\rho} + \vec{\beta}) \Delta z_m(\vec{\rho}) \right\} \quad (6.5)$$

gives the average relationship between the roughness functions Δz_n and Δz_m for interfaces n and m that are laterally separated by lag length $\vec{\beta}$. Note that in Equations 6.4 and 6.5, we have invoked the ergodic, stationary, and isotropic assumptions where $G_{nm}(\vec{\beta}) = G_{nm}(\beta)$ and $\beta = |\vec{\beta}|$.

We consider two separate cases regarding the correlation of the interface roughness between interfaces and these lead to different ARS results. In the first case, the roughness is literally identical at each interface and this is called a *correlated multilayer stack*. In the second case, the roughness at a given interface is statistically independent of the roughness at any other different interface and this is called an *uncorrelated multilayer stack*. The statistical relationship of the roughness between interfaces n and m is given by their cross-correlation function $G_{nm}(\beta)$ where $n \neq m$ or autocorrelation function $G_{nn}(\beta)$ when $m = n$.

We assume a functional form for the correlation function $G_{nm}(\beta)$ and calculate the corresponding power spectral density $g_{nm}(\vec{k}_0 - \vec{k})$ from Equation 6.4. In this study we assume for all interfaces n and m that the correlation functions for the *correlated* model can be written as

$$G_{nm}(\beta) = G(\beta) \quad (6.6a)$$

and this is rather obvious since all interfaces are identical. Thus, for this case, the auto- and cross-correlation functions are the same at and between all interfaces. In the case of the *uncorrelated* model, we assume

$$G_{nm}(\beta) = \delta_{nm} G(\beta) \quad (6.6b)$$

where the correlation function $G(\beta)$ is the same in both models. The only difference is that the cross-correlation function vanishes in the uncorrelated model. The correlated and uncorrelated models are perhaps the simplest to consider; however, more complicated modeling can be done, such as varying the degree of correlation between interfaces.

We write the correlation function $G(\beta)$ as a sum of an exponential and a Gaussian as

$$G(\beta) = \delta_L^2 e^{-|\beta|/\sigma_L} + \delta_S^2 e^{-\beta^2/\sigma_S^2} \quad (6.7)$$

which, when used in Equation 6.4, yields the power spectral density function $g(\vec{k}_0 - \vec{k})$ as

$$g(\vec{k}_0 - \vec{k}) = \frac{2\pi\delta_L^2\sigma_L^2}{[1 + |\vec{k}_0 - \vec{k}|^2\sigma_L^2]^{3/2}} + \pi\delta_S^2\sigma_S^2 e^{-|\vec{k}_0 - \vec{k}|^2/\sigma_S^2} \quad (6.8a)$$

where

$$|\vec{k}_0 - \vec{k}|^2 = k_0^2 + k^2 - 2k_0k \cos \phi \quad (6.8b)$$

The L and S subscripts refer to long- and short-range roughness scale, respectively. The δ_L and σ_L are the long-range rms roughness and correlation length, respectively, as the δ_S and σ_S are the short-range rms roughness and correlation length, respectively. With these assumptions the ARS formulas for the correlated model become

$$\frac{1}{P_0} \left\langle \frac{dP_{L+1}^{CORR}}{d\Omega} \right\rangle = \frac{(\omega/c)^2 q_{L+2}^{(1)} \epsilon_{L+2} \cos \theta}{(2\pi)^2 q_{L+2}^{(0)}} \left\{ \left| \sum_{j=1}^{L+1} A_j \right|^2 + \left| \sum_{j=1}^{L+1} G_j \right|^2 \right\} g(\vec{k}_0 - \vec{k}) \quad (6.9)$$

$$\frac{1}{P_0} \left\langle \frac{dP_1^{CORR}}{d\Omega} \right\rangle = \frac{(\omega/c)^2 q_1^{(1)} \epsilon_1 \cos \theta}{(2\pi)^2 q_{L+2}^{(0)}} \left\{ \left| \sum_{j=1}^{L+1} B_j \right|^2 + \left| \sum_{j=1}^{L+1} F_j \right|^2 \right\} g(\vec{k}_0 - \vec{k}) \quad (6.10)$$

The corresponding results for the uncorrelated model become

$$\frac{1}{P_0} \left\langle \frac{dP_{L+1}^{UNCORR}}{d\Omega} \right\rangle = \frac{(\omega/c)^2 q_{L+2}^{(1)} \epsilon_{L+2} \cos \theta}{(2\pi)^2 q_{L+2}^{(0)}} \left\{ \sum_{j=1}^{L+1} |A_j|^2 + \sum_{j=1}^{L+1} |G_j|^2 \right\} g(\vec{k}_0 - \vec{k}) \quad (6.11)$$

$$\frac{1}{P_0} \left\langle \frac{dP_1^{UNCORR}}{d\Omega} \right\rangle = \frac{(\omega/c)^2 q_1^{(1)} \epsilon_1 \cos \theta}{(2\pi)^2 q_{L+2}^{(0)}} \left\{ \sum_{j=1}^{L+1} |B_j|^2 + \sum_{j=1}^{L+1} |F_j|^2 \right\} g(\vec{k}_0 - \vec{k}) \quad (6.12)$$

where it is emphasized again that for transmission scattering we assume *a priori* that $\Im\{\epsilon_1\} = 0$ and $\Re\{\epsilon_1\} > 0$.

7. COMPUTER PROGRAM AND NUMERICAL EXAMPLES

This section describes how to use a computer program written to obtain numerical results from the preceding ARS formulas and discusses specific numerical examples of input and output data. Appendix A lists corresponding symbols used in the computer program and symbols used in the theory as given in the preceding sections. The computer code is given in Appendix B. In the computer algorithm, the $k_0, k, q_j^{(0)}$, and $q_j^{(1)}$ have been normalized to ω/c throughout. This is important to remember when trying to compare the previously outlined theory with the code. The computer code consists of a main program and one subroutine called "ZERO." The subroutine ZERO computes the zero-order field.

Taking into account normalization by ω/c as mentioned above, the ARS for reflection and transmission scattering as in Equations 6.9-6.12 are now rewritten as

$$\frac{1}{P_0} \left\langle \frac{dP_{L+2}^{CORR}}{d\Omega} \right\rangle = \frac{q_{L+2}^{(1)} \epsilon_{L+2} \cos \theta}{\lambda^2 q_{L+2}^{(0)}} \left\{ \left| \sum_{j=1}^{L+1} A_j \right|^2 + \left| \sum_{j=1}^{L+1} G_j \right|^2 \right\} g(\vec{k}_0 - \vec{k}) \quad (7.1)$$

$$\frac{1}{P_0} \left\langle \frac{dP_1^{CORR}}{d\Omega} \right\rangle = \frac{q_1^{(1)} \epsilon_1 \cos \theta}{\lambda^2 q_{L+2}^{(0)}} \left\{ \left| \sum_{j=1}^{L+1} B_j \right|^2 + \left| \sum_{j=1}^{L+1} F_j \right|^2 \right\} g(\vec{k}_0 - \vec{k}) \quad (7.2)$$

$$\frac{1}{P_0} \left\langle \frac{dP_{L+2}^{UNCORR}}{d\Omega} \right\rangle = \frac{q_{L+2}^{(1)} \epsilon_{L+2} \cos \theta}{\lambda^2 q_{L+2}^{(0)}} \left\{ \sum_{j=1}^{L+1} |A_j|^2 + \sum_{j=1}^{L+1} |G_j|^2 \right\} g(\vec{k}_0 - \vec{k}) \quad (7.3)$$

$$\frac{1}{P_0} \left\langle \frac{dP_1^{UNCORR}}{d\Omega} \right\rangle = \frac{q_1^{(1)} \epsilon_1 \cos \theta}{\lambda^2 q_{L+2}^{(0)}} \left\{ \sum_{j=1}^{L+1} |B_j|^2 + \sum_{j=1}^{L+1} |F_j|^2 \right\} g(\vec{k}_0 - \vec{k}) \quad (7.4)$$

where $\omega/c = 2\pi/\lambda$ has been used. In each of these four equations, the first summation in the $\{\dots\}$ brackets is the p-polarized component of the scattered field, whereas the second summation is the s-polarized field. Relating these formulas to the corresponding symbols in the computer code for p-polarized reflected and transmitted scattered light yields

$$\frac{1}{P_0} \left\langle \frac{dP_{L+2}^{CORR}}{d\Omega} \right\rangle = RPI(m) = \frac{q_{L+2}^{(1)} \epsilon_{L+2} \cos \theta}{\lambda^2 q_{L+2}^{(0)}} \left| \sum_{j=1}^{L+1} A_j \right|^2 g(\vec{k}_0 - \vec{k}) \quad (7.5)$$

$$\frac{1}{P_0} \left\langle \frac{dP_{L+2}^{UNCORR}}{d\Omega} \right\rangle = RP2(m) = \frac{q_{L+2}^{(1)} \epsilon_{L+1} \cos \theta^{L+1}}{\lambda^2 q_{L+2}^{(0)}} \sum_{j=1}^{L+1} |A_j|^2 g(\vec{k}_0 - \vec{k}) \quad (7.6)$$

$$\frac{1}{P_0} \left\langle \frac{dP_1^{CORR}}{d\Omega} \right\rangle = TP1(m) = \frac{q_1^{(1)} \epsilon_1 \cos \theta}{\lambda^2 q_{L+2}^{(0)}} \left| \sum_{j=1}^{L+1} B_j \right|^2 g(\vec{k}_0 - \vec{k}) \quad (7.7)$$

$$\frac{1}{P_0} \left\langle \frac{dP_1^{UNCORR}}{d\Omega} \right\rangle = TP2(m) = \frac{q_1^{(1)} \epsilon_1 \cos \theta^{L+1}}{\lambda^2 q_{L+2}^{(0)}} \sum_{j=1}^{L+1} |B_j|^2 g(\vec{k}_0 - \vec{k}) \quad (7.8)$$

The corresponding results for s-polarized reflected and transmitted scattered light are

$$\frac{1}{P_0} \left\langle \frac{dP_{L+2}^{CORR}}{d\Omega} \right\rangle = RS1(m) = \frac{q_{L+2}^{(1)} \epsilon_{L+1} \cos \theta}{\lambda^2 q_{L+2}^{(0)}} \left| \sum_{j=1}^{L+1} G_j \right|^2 g(\vec{k}_0 - \vec{k}) \quad (7.9)$$

$$\frac{1}{P_0} \left\langle \frac{dP_{L+1}^{UNCORR}}{d\Omega} \right\rangle = RS2(m) = \frac{q_{L+2}^{(1)} \epsilon_{L+2} \cos \theta^{L+1}}{\lambda^2 q_{L+2}^{(0)}} \sum_{j=1}^{L+1} |G_j|^2 g(\vec{k}_0 - \vec{k}) \quad (7.10)$$

$$\frac{1}{P_0} \left\langle \frac{dP_1^{CORR}}{d\Omega} \right\rangle = TS1(m) = \frac{q_1^{(1)} \epsilon_1 \cos \theta}{\lambda^2 q_{L+2}^{(0)}} \left| \sum_{j=1}^{L+1} F_j \right|^2 g(\vec{k}_0 - \vec{k}) \quad (7.11)$$

$$\frac{1}{P_0} \left\langle \frac{dP_1^{UNCORR}}{d\Omega} \right\rangle = TS2(m) = \frac{q_1^{(1)} \epsilon_1 \cos \theta^{L+1}}{\lambda^2 q_{L+2}^{(0)}} \sum_{j=1}^{L+1} |F_j|^2 g(\vec{k}_0 - \vec{k}) \quad (7.12)$$

The $RP1(m)$, $RP2(m)$, etc., are 1-D arrays for ARS at polar angle $X(m) = THETA = \theta$ where the integer $m = 1 \rightarrow NM$ and NM is the number of data points calculated. The R and T denote reflectance and transmitted ARS, respectively. The P and S refer to the scattered field polarization relative to the plane of scattering, respectively. Finally, The 1 and 2 signify that the multilayer stack is correlated or uncorrelated, respectively.

Some of the following statements reflect the fact that this FORTRAN code was run on the Naval Air Warfare Center Weapons Division's Cray supercomputer. Of course, a Cray is not needed since a VAX or PC with the necessary memory will suffice. To run this code requires input of data, which are read from a file called *nawc.in* along with consistent data in two PARAMETER statements. The PARAMETER statements are discussed in the next paragraph. There are four READ statements. The first statement reads, in degrees, the beginning (TS), ending (TF), and increment (DT) on scattering angle THETA. From these

three values, the number of data points NM is calculated. The second statement reads THETA0 (polar angle of incidence in degrees), LAMBDA (wavelength), PHI0 (azimuth angle defining scattering plane, in degrees), and L (number of layers in the multilayer stack). The third statement reads the rms roughness and correlation length values: RMSL,SIGL,RMSS,SIGS. The last READ statement reads in the multilayer stack design, layer by layer, as described by their complex dielectric constant and physical thickness. These data are read starting with the substrate, through the L layers in the stack, and ending with the superstrate. The program prompts the user for the unit number of the output data file. For example, if you enter "35" as the unit number, the output data is stored in "fort.35."

Sample input and output data files are given in Appendixes C through F. Also shown in each appendix are sample plots of ARS versus polar scattering angle THETA. The output data file lists the polarization angle of the incident beam PSI, the angles PHI0 and THETA0, and the wavelength (LAMBDA). Following this are ARS output data given in rows preceded by a P or S which denote the polarization of the *scattered* field for the data in that row. In rows preceded by a P follows the polar scattering angle THETA, correlated reflected ARS (RP1), uncorrelated reflected ARS (RP2), correlated transmitted ARS (TP1), and uncorrelated transmitted ARS (TP2). Similarly, in rows preceded by an S follows THETA, correlated reflected ARS (RS1), uncorrelated reflected ARS (RS2), correlated transmitted ARS (TS1), and uncorrelated transmitted ARS (TS2). Also shown in each appendix is the corresponding *nawc.in* input data file. THETA values are given as either positive or negative: positive values are for azimuth scattering angle $\text{PHI} = \text{PHI0}$; negative values are for azimuth scattering angle $\text{PHI} = \text{PHI0} + 180$ (degrees).

All numerical values given here used the same rms and correlation length values of $\text{RMSS} = 0.00049$ microns, $\text{SIGS} = 0.2$ microns, $\text{RMSL} = 0.0005$ microns, and $\text{SIGL} = 2.0$ microns.

Appendix C provides numerical input and output results for a 28-layer ($L = 28$) stack, angle of incidence $\text{THETA0} = 45.0$ degrees, azimuth angle $\text{PHI0} = 0.0$ degrees, and wavelength $\text{LAMBDA} = 0.65$ microns. The incident and substrate media dielectric constants are $E(30) = (1.0,0.0)$ and $E(1) = (2.3104,0.0)$, respectively. The complete design of the multilayer system is given in Appendix C. Shown in Figures C-1(a) through (d) are plots of reflected and transmitted ARS versus THETA for various polarizations and correlated or uncorrelated interface roughness.

Appendix D provides an example of input and output data for ARS from a bare ($L = 0$) surface that includes total internal reflection. The incident and substrate media have dielectric constants $E(2) = (4.41,0.0)$ and $E(1) = (1.0,0.0)$, respectively. The wavelength $\text{LAMBDA} = 0.633$ microns, azimuth angle $\text{PHI0} = 0.0$ degrees, and angle of incidence $\text{THETA0} = 35.0$ degrees, which is beyond the critical angle of 28.44 degrees. In this case

there is no specular transmitted beam but there is transmitted scattered light. Figures D-1(a) and (b) show reflected and transmitted ARS versus THETA for various polarizations. Since there is only one interface, the correlated and uncorrelated models give identical results.

Appendix E lists numerical input and output data for an example of out-of-plane ARS where the azimuth angle $\text{PHI0} = 35.0$ degrees, angle of incidence $\text{THETA0} = 60.0$ degrees, and wavelength $\text{LAMBDA} = 0.633$ microns. The stack has five layers ($L = 5$) and an absorbing metallic substrate. In this case there is no transmitted scattered light, and the multilayer design is given in the appendix. Figures E-1(a) through (d) plot reflected ARS versus THETA for all permutations of p- and s-polarization of the incident and scattered light. Also, ARS for both correlated and uncorrelated roughness is shown.

Appendix F provides a final example of input and output data for a single layer case ($L = 1$) where the incident medium is $E(3) = (4.41, 0.0)$, followed by a partially opaque 0.025-micron-thick metal film with dielectric constant $E(2) = (-16.0, 0.5)$ and an air substrate with $E(1) = (1.0, 0.0)$. The wavelength $\text{LAMBDA} = 0.633$ microns, $\text{THETA0} = 29.6$ degrees, and $\text{PHI0} = 0.0$ degrees. This case is of interest because, for p-polarized incident light at this angle of incidence, direct coupling to a surface plasma resonance in the metal film does occur and this has an effect on the resulting scattered light. Figures F-1(a) through (d) show plots of reflected and transmitted ARS versus THETA for p- and s-polarization of the incident and scattered fields.

8. REFERENCES

1. Air Force Weapons Laboratory. *Low Efficiency Diffraction Grating Theory*, by J. M. Elson. Kirtland Air Force Base, N. Mex., March 1976. (AFWL-TR-75-210, publication UNCLASSIFIED.); J. M. Elson. "Angle-Resolved Light Scattering From Composite Optical Surfaces," *Proc. SPIE*, Vol. 240 (29 July-1 August 1980), pp. 296-305.
2. J. M. Elson, J. P. Rahn, and J. M. Bennett. "Relationship of the Total Integrated Scattering From Multilayer-Coated Optics to Angle of Incidence, Polarization, Correlation Length, and Roughness Cross-Correlation Properties," *Appl. Opt.*, Vol. 22 (1983), pp. 3207-3219.
3. E. Kroger and E. Kretschmann. "Scattering of Light by Slightly Rough Surfaces or Thin Films Including Plasma Resonance Emission," *Z. Physik*, Vol. 237 (1970), pp. 1-15.

Appendix A
CORRESPONDENCE BETWEEN SYMBOLS USED IN THE
COMPUTER CODE AND THEORY

Listed below are the symbol relationships between the computer listing in Appendix B and the theory as discussed in the main body of this publication.

$\lambda =$	LAMBDA	$Y_{1,j}^{(0)} =$	Y1(j)	$P_{0,11}^{(1,j)} =$	P011(j)
$k =$	K	$Y_{2,j}^{(0)} =$	Y2(j)	$P_{0,12}^{(1,j)} =$	P012(j)
$k_0 =$	K0	$X_j^{(0)} =$	X0(j)	$P_{0,21}^{(1,j)} =$	P021(j)
$d_j =$	D(j)	$\xi_1^{(1,j-1)} =$	XI1(j)	$P_{0,22}^{(1,j)} =$	P022(j)
$\tau_j =$	T(j)	$\xi_2^{(1,j-1)} =$	XI2(j)	$S_{0,11}^{(1,j)} =$	S011(j)
$\epsilon_j =$	E(j)	$\eta_1^{(1,j-1)} =$	ETA1(j)	$S_{0,12}^{(1,j)} =$	S012(j)
$\theta_0 =$	THETA0	$\eta_2^{(1,j-1)} =$	ETA2(j)	$S_{0,21}^{(1,j)} =$	S021(j)
$\theta =$	THETA	$\eta_3^{(1,j-1)} =$	ETA3(j)	$S_{0,22}^{(1,j)} =$	S022(j)
$\phi =$	PHI	$\eta_4^{(1,j-1)} =$	ETA4(j)	$P_{1,11}^{(1,j)} =$	P11(j)
$\sigma_L =$	SIGL	$\mu_1^{(1,j-1)} =$	MU1(j)	$P_{1,12}^{(1,j)} =$	P12(j)
$\delta_L =$	RMSL	$\mu_2^{(1,j-1)} =$	MU2(j)	$P_{1,21}^{(1,j)} =$	P21(j)
$\sigma_s =$	SIGS	$q_j^{(0)} =$	Q0(j)	$P_{1,22}^{(1,j)} =$	P22(j)
$\delta_s =$	RMSS	$q_j^{(1)} =$	Q1(j)	$S_{1,11}^{(1,j)} =$	S11(j)
$\omega/c =$	WC	$e_{j,x}^{(0)}(d_j) =$	E0X(j)	$S_{1,12}^{(1,j)} =$	S12(j)
$\psi =$	PSI	$e_{j,y}^{(0)}(d_j) =$	E0Y(j)	$S_{1,21}^{(1,j)} =$	S21(j)
$ \vec{k}_0 - \vec{k} =$	DELK	$e_{j,z}^{(0)}(d_j) =$	E0Z(j)	$S_{1,22}^{(1,j)} =$	S22(j)
$g(\vec{k}_0 - \vec{k}) =$	GK	$a_j^{(0)} =$	A0(j)	$R_p =$	RP
$a_j^{(1)} =$	AJ	$b_j^{(0)} =$	B0(j)	$T_p =$	TP
$b_j^{(1)} =$	BJ	$f_j^{(0)} =$	F0(j)	$R_s =$	RS
$f_j^{(1)} =$	FJ	$g_j^{(0)} =$	G0(j)	$T_s =$	TS
$g_j^{(1)} =$	GJ				

Appendix B

FORTRAN LISTING OF MULTILAYER SCATTERING SOURCE CODE

```

C THIS PROGRAM IS DESIGNED TO PREDICT ANGLE RESOLVED
C SCATTERING (ARS) DUE TO ROUGHNESS PRESENT AT THE INTERFACES
C OF MULTILAYERED OPTICAL SURFACES. THE SCATTERING IS
C CALCULATED AS A REFLECTED OR TRANSMITTED FIELD. IT IS
C VALID ONLY WHEN THE RMS ROUGHNESS VALUES OF THE
C INTERFACES ARE MUCH LESS THAN THE INCIDENT WAVELENGTH.
C THE PROGRAM AS WRITTEN HERE CONSIDERS THE CASES OF (1)
C IDENTICAL ROUGHNESS AT EACH INTERFACE (CORRELATED),
C (2) INDEPENDENT ROUGHNESS BETWEEN DIFFERENT INTERFACES,
C (UNCORRELATED), AND (3) A PARTIALLY CORRELATED MODEL. THE
C PARTIAL CORRELATION MODEL ASSUMES THAT THE LONG-RANGE-
C SCALE ROUGHNESS IS CORRELATED BETWEEN INTERFACES AND
C THE SHORT-RANGE-SCALE ROUGHNESS IS UNCORRELATED BETWEEN
C INTERFACES. THE OUTPUT IS THE ARS, i. e., SCATTERED POWER
C PER UNIT SOLID ANGLE NORMALIZED TO THE INCIDENT POWER
C VERSUS POLAR ANGLE OF SCATTERING. FOR REFLECTION
C SCATTERING, THE POLAR SCATTERING ANGLE IS IN THE INCIDENT
C MEDIUM. FOR TRANSMISSION SCATTERING, THE POLAR SCATTERING
C ANGLE IS IN THE SUBSTRATE MEDIUM.
C
C NL = L + 2 (SEE MAIN PROGRAM AND SUBROUTINE "ZERO")
C NP = MAXIMUM NUMBER OF OUTPUT DATA POINTS TO CALCULATE
C
C IN THE PARAMETER STATEMENT OF THE FOLLOWING PROGRAM LISTING,
C THE NUMBER OF LAYERS, L = 5, AND THUS NL = 7.

```

```

PARAMETER(NP = 400,NL = 7)
DIMENSION X(NP)
COMPLEX XI1(0:NL) , XI2(0:NL) , MU1(0:NL) , MU2(0:NL)
COMPLEX ETA1(0:NL) , ETA2(0:NL)
COMPLEX ETA3(0:NL) , ETA4(0:NL)
COMPLEX P11(0:NL) , P12(0:NL) , P21(0:NL) , P22(0:NL)
COMPLEX S11(0:NL) , S12(0:NL) , S21(0:NL) , S22(0:NL)
COMPLEX E(NL) , Q0(NL) , Q1(NL)
COMPLEX PP , PM , SP , SM , Z11 , Z12 , Z21 , Z22
COMPLEX I , Z , Z1 , Z2 , Z3 , Z4 , ZU , ZB , ZE
COMPLEX ZUM1 , ZUM2 , ZUM3 , ZUM4
COMPLEX AJ , BJ , FJ , GJ
COMPLEX Y11 , Y12 , Y21 , Y22
COMPLEX X11 , X12 , X21 , X22
COMPLEX Y1(NL) , Y2(NL) , X0(NL)
COMPLEX E0X(NL) , E0Z(NL) , E0Y(NL)
REAL LAMBDA , K , K0
REAL D(NL) , T(NL)
REAL SUM1 , SUM2
REAL RP1(NP) , RS1(NP) , RP2(NP)
REAL RS2(NP) , RP3(NP) , RS3(NP)

```

NAWCWPNS TP 8084

```

REAL TP1(NP) , TS1(NP) , TP2(NP)
REAL TS2(NP) , TP3(NP) , TS3(NP)
INTEGER NM

OPEN(unit = 20, file = 'nawc.in' , status = 'old')
READ(20,*) TS,TF,DT
READ(20,*) THETA0,LAMBDA,PHI0,L
READ(20,*) RMSL,SIGL,RMSS,SIGS

PI = ACOS(-1.0)
L1 = L + 1
L2 = L + 2
WC = 2*PI/LAMBDA
I = (0.0 , 1.0)
DR = PI/180.

READ(20,*) (E(M),T(M), M = 1, L2)

C INPUT PARAMETERS:
C TS = START VALUE (DEG) OF POLAR SCATTERING ANGLE THETA
C TF = FINAL VALUE (DEG) OF POLAR SCATTERING ANGLE THETA
C DT = INCREMENT ON POLAR ANGLE THETA (DEGREES)
C THETA0 = ANGLE OF INCIDENCE (DEG) MEASURED FROM THE NORMAL
C PHI0 = AZIMUTHAL SCATTERING ANGLE DESIRED (DEG). FOR
C EXAMPLE, IF YOU WANT TO LOOK AT SCATTERING IN THE PLANE OF
C INCIDENCE, SET PHI0 = 0. THIS PROGRAM AUTOMATICALLY SHIFTS
C PHI0 180 DEGREES FOR SCATTERING IN THE QUADRANT CONTAINING
C THE INCOMING BEAM.
C LAMBDA = INCIDENT WAVELENGTH
C L = INTEGER NUMBER OF LAYERS IN MULTILAYER STACK
C
C E(J) = COMPLEX DIELECTRIC CONSTANT ARRAY
C
C   E(1) = SUBSTRATE
C   E(2) = FIRST LAYER
C   .
C   .
C   E(L+1) = OUTERMOST LAYER
C   E(L+2) = REGION ABOVE STACK - SUPERSTRATE
C
C T(J): THICKNESSES OF THE ITH LAYER
C
C   T(1) = NOT USED
C   T(2) PHYSICAL THICKNESS OF LAYER NEXT TO SUBSTRATE
C   .
C   .
C   T(L+1) = OUTERMOST LAYER PHYSICAL THICKNESS
C   T(L+2) = NOT USED
C
C   D(1) = 0.0
C D(J) = ABSOLUTE THICKNESS OF MULTILAYER STACK AT INTERFACE J
C   IF(L.GT.0) THEN
C     DO 706 J = 2 , L1
706   D(J) = D(J-1) + T(J)
C     ELSE IF(L.EQ.0) THEN
C       ENDIF
C
C NM,LE,NP IS THE CALCULATED NUMBER OF OUTPUT DATA POINTS

```

NAWCWPNS TP 8084

```

XM = (TF - TS)/DT + 1.0
NM = INT(XM) + 1
1001 CONTINUE
K0 = SQRT(REAL(E(L2)))*SIN(DR*THETA0)
DO 301 J = 1 , L2
301 Q0(J) = CSQRT(E(J) - K0**2)
CALL ZERO(E0X,E0Z,E0Y,Q0,E,D,K0,L,WC)
NIJ = 2
IF(REAL(E(1)).LE.0.0) NIJ = 1
DO 121 JJ = 1, 2
C TWO VALUES OF POLARIZATION ANGLE SIGMA ARE USED, BUT
C ANY RANGE OF VALUES (IN RADIANS) MAY BE USED
C
C WHEN JJ = 1 -> P-POLARIZED INCIDENT BEAM
C WHEN JJ = 2 -> S-POLARIZED INCIDENT BEAM
C
SIGMA = (JJ - 1)*(PI/2.)
POC = COS(SIGMA)
POS = SIN(SIGMA)
DO 122 IJ = 1, NIJ
C WHEN IJ = 1 -> REFLECTION SCATTERING
C WHEN IJ = 2 -> TRANSMISSION SCATTERING
C IF(REAL(E(1)).LE.0.0) TRANSMISSION SCATTERING IS OMITTED
C
DO 120 II = 1 , NM
C THETA = POLAR ANGLE OF SCATTERING
THETA = TS + (II - 1)*DT
X(II) = THETA
C NOTE DIFFERENT K FOR REFLECTION (IJ=1) AND TRANSMISSION (IJ=2) SCATTERING
IF(IJ.EQ.1) THEN
K = SQRT(REAL(E(L2)))*ABS(SIN(DR*THETA))
ELSE IF(IJ.EQ.2) THEN
K = SQRT(REAL(E(1)))*ABS(SIN(DR*THETA))
ENDIF
C PHI = AZIMUTHAL ANGLE OF SCATTERING
C IF SIGN OF THETA POSITIVE, PHI = PHI0
C IF SIGN OF THETA NEGATIVE, PHI = PHI0 + 180
IF(THETA.LT.0.) PHI = DR*(PHI0 + 180.)
IF(THETA.GE.0.) PHI = DR*PHI0
AZC = COS(PHI)
AZS = SIN(PHI)
DO 310 J = 1 , L2
310 Q1(J) = CSQRT(E(J) - K**2)
C SOURCE TERMS
DO 302 J = 1 , L1
ZE = E(J+1) - E(J)
Y1(J) = I*WC*ZE*K*E0Z(J)*POC/E(J+1)
Y2(J) = I*WC*ZE*(E0X(J)*AZC*POC + E0Y(J)*AZS*POS)
X0(J) = I*WC*ZE*(E0X(J)*AZS*POC - E0Y(J)*AZC*POS)

```

NAWCWPNS TP 8084

302 CONTINUE

$Y11 = (1.,0.)$
 $Y12 = (0.,0.)$
 $Y21 = (0.,0.)$
 $Y22 = (1.,0.)$
 $X11 = (1.,0.)$
 $X12 = (0.,0.)$
 $X21 = (0.,0.)$
 $X22 = (1.,0.)$
 DO 311 M = 1 , L1
 $ZB = I*WC*(Q1(M+1) - Q1(M))*D(M)$
 $ZU = I*WC*(Q1(M+1) + Q1(M))*D(M)$
 $Z = CSQRT(E(M)*E(M+1))$
 $PP = (Q1(M+1)*E(M) + Q1(M)*E(M+1))/(2*Q1(M)*Z)$
 $PM = (Q1(M+1)*E(M) - Q1(M)*E(M+1))/(2*Q1(M)*Z)$
 $Z11 = PP*CEXP(ZB)$
 $Z12 = PM*CEXP(-ZU)$
 $Z21 = PM*CEXP(ZU)$
 $Z22 = PP*CEXP(-ZB)$
 $P11(M) = Y11*Z11 + Y12*Z21$
 $P12(M) = Y11*Z12 + Y12*Z22$
 $P21(M) = Y21*Z11 + Y22*Z21$
 $P22(M) = Y21*Z12 + Y22*Z22$
 $Y11 = P11(M)$
 $Y12 = P12(M)$
 $Y21 = P21(M)$
 $Y22 = P22(M)$
 $SP = (Q1(M) + Q1(M+1))/(2*Q1(M))$
 $SM = (Q1(M) - Q1(M+1))/(2*Q1(M))$
 $Z11 = SP*CEXP(ZB)$
 $Z12 = SM*CEXP(-ZU)$
 $Z21 = SM*CEXP(ZU)$
 $Z22 = SP*CEXP(-ZB)$
 $S11(M) = X11*Z11 + X12*Z21$
 $S12(M) = X11*Z12 + X12*Z22$
 $S21(M) = X21*Z11 + X22*Z21$
 $S22(M) = X21*Z12 + X22*Z22$
 $X11 = S11(M)$
 $X12 = S12(M)$
 $X21 = S21(M)$
 $X22 = S22(M)$

311 CONTINUE

$P11(0) = (1.,0.)$
 $P12(0) = (0.,0.)$
 $P21(0) = (0.,0.)$
 $P22(0) = (1.,0.)$
 $S11(0) = (1.,0.)$
 $S12(0) = (0.,0.)$
 $S21(0) = (0.,0.)$
 $S22(0) = (1.,0.)$
 DO 300 J = 0, L

NAWCWPNS TP 8084

```

Z1 = CEXP(-I*WC*Q1(J+1)*D(J+1))
Z2 = CEXP( I*WC*Q1(J+1)*D(J+1))

ETA1(J) = P11(J)*Z1 + P12(J)*Z2
ETA2(J) = P11(J)*Z1 - P12(J)*Z2
ETA3(J) = P21(J)*Z1 + P22(J)*Z2
ETA4(J) = P21(J)*Z1 - P22(J)*Z2

XI1(J) = S11(J)*Z1 - S12(J)*Z2
XI2(J) = S21(J)*Z1 - S22(J)*Z2

MU1(J) = P11(L1)*ETA3(J) - P21(L1)*ETA1(J)
MU2(J) = P11(L1)*ETA4(J) - P21(L1)*ETA2(J)

300 CONTINUE

ARG = K**2 + K0**2 - 2*K*K0*AZC
IF(ARG.LE.0.) DELK = 0.
IF(ARG.GT.0.) DELK = SQRT(ARG)
DELK = WC*DELK

C
C THIS PROGRAM ASSUMES A TWO PART AUTOCORRELATION FUNCTION
C (ACF):
C   ACF = EXPONENTIAL + GAUSSIAN
C
C THE RESULTING SPECTRAL DENSITY FUNCTION NEEDS FOUR (4) INPUT
C PARAMETERS.
C
C   RMSL = LONG-RANGE ROUGHNESS RMS VALUE
C   RMSS = SHORT-RANGE ROUGHNESS RMS VALUE
C   SIGL = LONG-RANGE ROUGHNESS CORRELATION LENGTH
C   SIGS = SHORT-RANGE ROUGHNESS CORRELATION LENGTH
C
GKL = 2*PI*(RMSL*SIGL)**2/((1.+(SIGL*DELK)**2)**1.5)
GKS = PI*(RMSS*SIGS)**2*EXP(-(SIGS*DELK/2.))**2)
GK = GKS + GKL

ZUM1 = (0.0,0.0)
ZUM2 = (0.0,0.0)
ZUM3 = (0.0,0.0)
ZUM4 = (0.0,0.0)
SUM1 = 0.0
SUM2 = 0.0
SUM3 = 0.0
SUM4 = 0.0

DO 313 J = 1, L1
C ZUM1 = SUM FOR P-POL SCATTERED, CORRELATED, REFLECTED
C SUM1 = SUM FOR P-POL SCATTERED, UNCORRELATED, REFLECTED
Z = CSQRT(E(J))
AJ = (Z*Y1(J)*ETA1(J-1)/Q1(J) - Y2(J)*ETA2(J-1)/Z)/(2*P11(L1))
ZUM1 = ZUM1 + AJ
SUM1 = SUM1 + (CABS(AJ))**2
C ZUM2 = SUM FOR S-POL SCATTERED, CORRELATED, REFLECTED
C SUM2 = SUM FOR S-POL SCATTERED, UNCORRELATED, REFLECTED
GJ = -X0(J)*XI1(J-1)/(2*Q1(J)*S11(L1))
ZUM2 = ZUM2 + GJ
SUM2 = SUM2 + (CABS(GJ))**2
C ZUM3 = SUM FOR P-POL SCATTERED, CORRELATED, TRANSMITTED
C SUM3 = SUM FOR P-POL SCATTERED, UNCORRELATED, TRANSMITTED

```

NAWCWPNS TP 8084

```

BJ = -(Z*Y1(J)*MU1(J-1)/Q1(J) - Y2(J)*MU2(J-1)/Z)/(2*P11(L1))
ZUM3 = ZUM3 + BJ
SUM3 = SUM3 + (CABS(BJ))**2
C ZUM4 = SUM FOR S-POL SCATTERED, CORRELATED, TRANSMITTED
C SUM4 = SUM FOR S-POL SCATTERED, UNCORRELATED, TRANSMITTED
FJ = X0(J)*(S11(L1)*XI2(J-1) - S21(L1)*XI1(J-1))/(2*Q1(J)*S11(L1))
ZUM4 = ZUM4 + FJ
SUM4 = SUM4 + (CABS(FJ))**2

313 CONTINUE
Z = (Q1(L2)/Q0(L2))*(E(L2)/LAMBDA**2)*COS(DR*THETA)
CR = REAL(Z)
Z = (Q1(1)/Q0(L2))*(E(1)/LAMBDA**2)*COS(DR*THETA)
CT = REAL(Z)
IF(IJ.EQ.1) THEN
  RP1(II) = CR*(CABS(ZUM1))**2
  RP2(II) = CR*SUM1
C RP3 IS PARTIALLY CORRELATED MODEL
  RP3(II) = GKL*RP1(II) + GKS*RP2(II)
  RP1(II) = GK*RP1(II)
  RP2(II) = GK*RP2(II)
  RS1(II) = CR*(CABS(ZUM2))**2
  RS2(II) = CR*SUM2
C RS3 IS PARTIALLY CORRELATED MODEL
  RS3(II) = GKL*RS1(II) + GKS*RS2(II)
  RS1(II) = GK*RS1(II)
  RS2(II) = GK*RS2(II)
  ELSE IF(IJ.EQ.2) THEN
    TP1(II) = CT*(CABS(ZUM3))**2
    TP2(II) = CT*SUM3
C TP3 IS PARTIALLY CORRELATED MODEL
    TP3(II) = GKL*TP1(II) + GKS*TP2(II)
    TP1(II) = GK*TP1(II)
    TP2(II) = GK*TP2(II)
    TS1(II) = ABS(CT*(CABS(ZUM4))**2)
    TS2(II) = ABS(CT*SUM4)
C TS3 IS PARTIALLY CORRELATED MODEL
    TS3(II) = GKL*TS1(II) + GKS*TS2(II)
    TS1(II) = GK*TS1(II)
    TS2(II) = GK*TS2(II)
  ENDIF
120 CONTINUE
122 CONTINUE
WRITE(IUNIT,54)
PRINT*, 'POLARIZATION ANGLE SIGMA = ',SIGMA*180/PI, ' DEGREES'
PRINT*, ' DATA OUTPUT UNIT NUMBER ? '
READ*,IUNIT
WRITE(IUNIT,55)
WRITE(IUNIT,50) SIGMA*180/PI,LAMBDA
WRITE(IUNIT,51) THETA0,PHI0
WRITE(IUNIT,54)

```

NAWCWPNS TP 8084

```

WRITE(IUNIT,11)
WRITE(IUNIT,12)
WRITE(IUNIT,54)

DO 446 J = 1, NM
WRITE(IUNIT,9) X(J),RP1(J),RP2(J),TP1(J),TP2(J)
WRITE(IUNIT,10) X(J),RS1(J),RS2(J),TS1(J),TS2(J)
446 CONTINUE
121 CONTINUE

9 FORMAT(' P',F10.2,4E12.4)
10 FORMAT(' S',F10.2,4E12.4)
11 FORMAT(' ',1X,'THETA',5X,'RP1',9X,'RP2',9X,'TP1',9X,'TP2')
12 FORMAT(' ',1X,'THETA',5X,'RS1',9X,'RS2',9X,'TS1',9X,'TS2')
50 FORMAT(' SIGMA =',F10.2,' LAMBDA =',F8.4)
51 FORMAT(' THETA0 =',F10.2,' PHIO =',F8.2)
54 FORMAT(' ')
55 FORMAT(' *****')
STOP
END

C*****
C*****

SUBROUTINE ZERO(E0X,E0Z,E0Y,Q0,E,D,K0,L,WC)
C NL = NUMBER OF LAYERS(L) + 2 SHOULD MATCH MAIN PROGRAM

PARAMETER(NL = 7)
COMPLEX Q0(NL),E(NL),E0X(NL),E0Z(NL),E0Y(NL)
COMPLEX A0(NL),B0(NL),G0(NL),F0(NL)
COMPLEX X11,X12,X21,X22
COMPLEX Y11,Y12,Y21,Y22
COMPLEX S011(0:NL),S012(0:NL)
COMPLEX S021(0:NL),S022(0:NL)
COMPLEX P011(0:NL),P012(0:NL)
COMPLEX P021(0:NL),P022(0:NL)
COMPLEX PP,PM,SP,SM,Z11,Z12,Z21,Z22
COMPLEX I,Z,Z1,Z2,ZU,ZB
REAL WC,K0,RP,TP,RS,TS,D(NL)
INTEGER L,L1,L2

I = (0.0,1.0)
L1 = L + 1
L2 = L + 2

Y11 = (1.,0.)
Y12 = (0.,0.)
Y21 = (0.,0.)
Y22 = (1.,0.)

X11 = (1.,0.)
X12 = (0.,0.)
X21 = (0.,0.)
X22 = (1.,0.)

DO 311 M = 1, L1
ZB = I*WC*(Q0(M+1) - Q0(M))*D(M)
ZU = I*WC*(Q0(M+1) + Q0(M))*D(M)
Z = CSQRT(E(M)*E(M+1))

PP = (Q0(M+1)*E(M) + Q0(M)*E(M+1))/(2*Q0(M)*Z)
PM = (Q0(M+1)*E(M) - Q0(M)*E(M+1))/(2*Q0(M)*Z)

```

NAWCWPNS TP 8084

Z11 = PP*CEXP(ZB)
 Z12 = PM*CEXP(-ZU)
 Z21 = PM*CEXP(ZU)
 Z22 = PP*CEXP(-ZB)

P011(M) = Y11*Z11 + Y12*Z21
 P012(M) = Y11*Z12 + Y12*Z22
 P021(M) = Y21*Z11 + Y22*Z21
 P022(M) = Y21*Z12 + Y22*Z22

Y11 = P011(M)
 Y12 = P012(M)
 Y21 = P021(M)
 Y22 = P022(M)

SP = (Q0(M) + Q0(M+1))/(2*Q0(M))
 SM = (Q0(M) - Q0(M+1))/(2*Q0(M))

Z11 = SP*CEXP(ZB)
 Z12 = SM*CEXP(-ZU)
 Z21 = SM*CEXP(ZU)
 Z22 = SP*CEXP(-ZB)

S011(M) = X11*Z11 + X12*Z21
 S012(M) = X11*Z12 + X12*Z22
 S021(M) = X21*Z11 + X22*Z21
 S022(M) = X21*Z12 + X22*Z22

X11 = S011(M)
 X12 = S012(M)
 X21 = S021(M)
 X22 = S022(M)

311 CONTINUE

P011(0) = (1.,0.)
 P012(0) = (0.,0.)
 P021(0) = (0.,0.)
 P022(0) = (1.,0.)

S011(0) = (1.,0.)
 S012(0) = (0.,0.)
 S021(0) = (0.,0.)
 S022(0) = (1.,0.)

DO 104 J = 0, L1

A0(J+1) = -Q0(L2)*P012(J)/(P011(L1)*Q0(J+1))

B0(J+1) = Q0(L2)*P011(J)/(P011(L1)*Q0(J+1))

F0(J+1) = Q0(L2)*S011(J)/(S011(L1)*Q0(J+1))

G0(J+1) = -Q0(L2)*S012(J)/(S011(L1)*Q0(J+1))

104 CONTINUE

C INCIDENT FIELD COMPONENTS EVALUATED AT D(J)

DO 110 J = 1, L1

Z1 = CEXP(I*WC*Q0(J)*D(J))

Z2 = CEXP(-I*WC*Q0(J)*D(J))

Z = CSQRT(E(J))

E0X(J) = Q0(J)*(A0(J)*Z1 + B0(J)*Z2)/Z

E0Y(J) = -G0(J)*Z1 - F0(J)*Z2

E0Z(J) = -K0*(A0(J)*Z1 - B0(J)*Z2)/Z

110 CONTINUE

NAWCWPNS TP 8084

C SPECULAR REFLECTANCE

RP = (CABS(A0(L2)))**2

RS = (CABS(G0(L2)))**2

C SPECULAR TRANSMISSION

TP = REAL(Q0(1)/Q0(L2))*(CABS(B0(1)))**2

TS = REAL(Q0(1)/Q0(L2))*(CABS(F0(1)))**2

SUMS = RS + TS

SUMP = RP + TP

IF(SUMS.GT.1.001.OR.SUMP.GT.1.001) THEN

PRINT*, 'SUM OF ZERO-ORDER ENERGY GREATER THAN UNITY '

PRINT*, 'SUMP = ', SUMP, ' SUMS = ', SUMS

ELSE

RETURN

ENDIF

RETURN

END

Appendix C

INPUT DATA AND OUTPUT RESULTS FOR REFLECTION AND TRANSMISSION ARS FROM A MULTILAYER STACK WITH 28 LAYERS

OUTPUT DATA FILE:

SIGMA = 00.00 LAMBDA = 0.65
 THETA0 = 45.00 PHI0 = 0.00

THETA RP1 RP2 TP1 TS1
 THETA RS1 RS2 TP2 TS2

P ⇒ p-POL scatt. S ⇒ s-POL scatt.

INPUT DATA FILE:

-80.,80.,20.
 45.,0.65,0.0,28
 .0005,2.0.,.00049,0.2
 (2.3104,0.0),0.0
 (4.41,0.0),0.07738
 (2.1316,0.0),0.1113
 (4.41,0.0),0.07738
 (2.1316,0.0),0.1113
 (4.41,0.0),0.07738
 (2.1316,0.0),0.1113
 (4.41,0.0),0.30952
 (2.1316,0.0),0.1113
 (4.41,0.0),0.07738

P	-80.00	0.5510E-06	0.2279E-06	0.1392E-06	0.4680E-06
S	-80.00	0.7422E-34	0.1363E-33	0.6056E-35	0.2224E-34
P	-60.00	0.5691E-05	0.1488E-05	0.2453E-07	0.1772E-05
S	-60.00	0.1993E-33	0.5344E-33	0.9153E-33	0.3348E-33
P	-40.00	0.1307E-04	0.5629E-05	0.3252E-05	0.1223E-05
S	-40.00	0.4719E-33	0.7617E-33	0.1669E-34	0.9735E-35
P	-20.00	0.4870E-04	0.1396E-04	0.4698E-06	0.3695E-06
S	-20.00	0.3651E-32	0.1595E-32	0.2313E-34	0.2199E-34
P	0.00	0.4693E-04	0.3396E-04	0.8650E-04	0.7576E-04
S	0.00	0.0000E+00	0.0000E+00	0.0000E+00	0.0000E+00
P	20.00	0.1020E-03	0.5574E-04	0.5603E-05	0.5919E-05
S	20.00	0.0000E+00	0.0000E+00	0.0000E+00	0.0000E+00
P	40.00	0.6168E-03	0.1823E-02	0.4575E-04	0.3884E-04
S	40.00	0.0000E+00	0.0000E+00	0.0000E+00	0.0000E+00
P	60.00	0.1016E-03	0.9758E-04	0.1352E-05	0.4601E-04
S	60.00	0.0000E+00	0.0000E+00	0.0000E+00	0.0000E+00

SIGMA = 90.00 LAMBDA = 0.65
 THETA0 = 45.00 PHI0 = 0.00

THETA RP1 RP2 TP1 TS1
 THETA RS1 RS2 TP2 TS2

(2.1316,0.0),0.1113
 (4.41,0.0),0.07738
 (2.1316,0.0),0.1113
 (4.41,0.0),0.07738
 (2.1316,0.0),0.1113
 (4.41,0.0),0.07738
 (2.1316,0.0),0.1113
 (4.41,0.0),0.07738
 (2.1316,0.0),0.1113
 (4.41,0.0),0.07738
 (2.1316,0.0),0.1113
 (4.41,0.0),0.07738
 (2.1316,0.0),0.1113
 (4.41,0.0),0.10369
 (2.1316,0.0),0.14469
 (1.00,0.),0.0

P	-80.00	0.8865E-34	0.5082E-34	0.7981E-35	0.7769E-34
S	-80.00	0.2955E-06	0.1567E-05	0.7331E-07	0.1581E-06
P	-60.00	0.6772E-33	0.3114E-33	0.4268E-36	0.3414E-33
S	-60.00	0.7810E-06	0.6234E-05	0.6857E-05	0.2264E-05
P	-40.00	0.1651E-32	0.1733E-32	0.5596E-33	0.2206E-33
S	-40.00	0.2238E-05	0.8541E-05	0.2812E-07	0.4702E-07
P	-20.00	0.7515E-32	0.3610E-32	0.4698E-34	0.5450E-34
S	-20.00	0.1810E-04	0.1409E-04	0.3415E-07	0.5619E-07
P	0.00	0.1364E-32	0.9866E-33	0.2513E-32	0.2201E-32
S	0.00	0.2432E-04	0.3003E-04	0.5186E-04	0.6718E-04
P	20.00	0.2965E-32	0.1619E-32	0.1628E-33	0.1720E-33
S	20.00	0.6900E-04	0.5369E-04	0.6423E-06	0.1057E-05
P	40.00	0.1792E-31	0.5298E-31	0.1329E-32	0.1128E-32
S	40.00	0.6030E-03	0.2302E-02	0.8518E-06	0.1425E-05
P	60.00	0.2953E-32	0.2835E-32	0.3929E-34	0.1337E-32
S	60.00	0.5248E-04	0.4189E-03	0.2260E-03	0.7461E-04

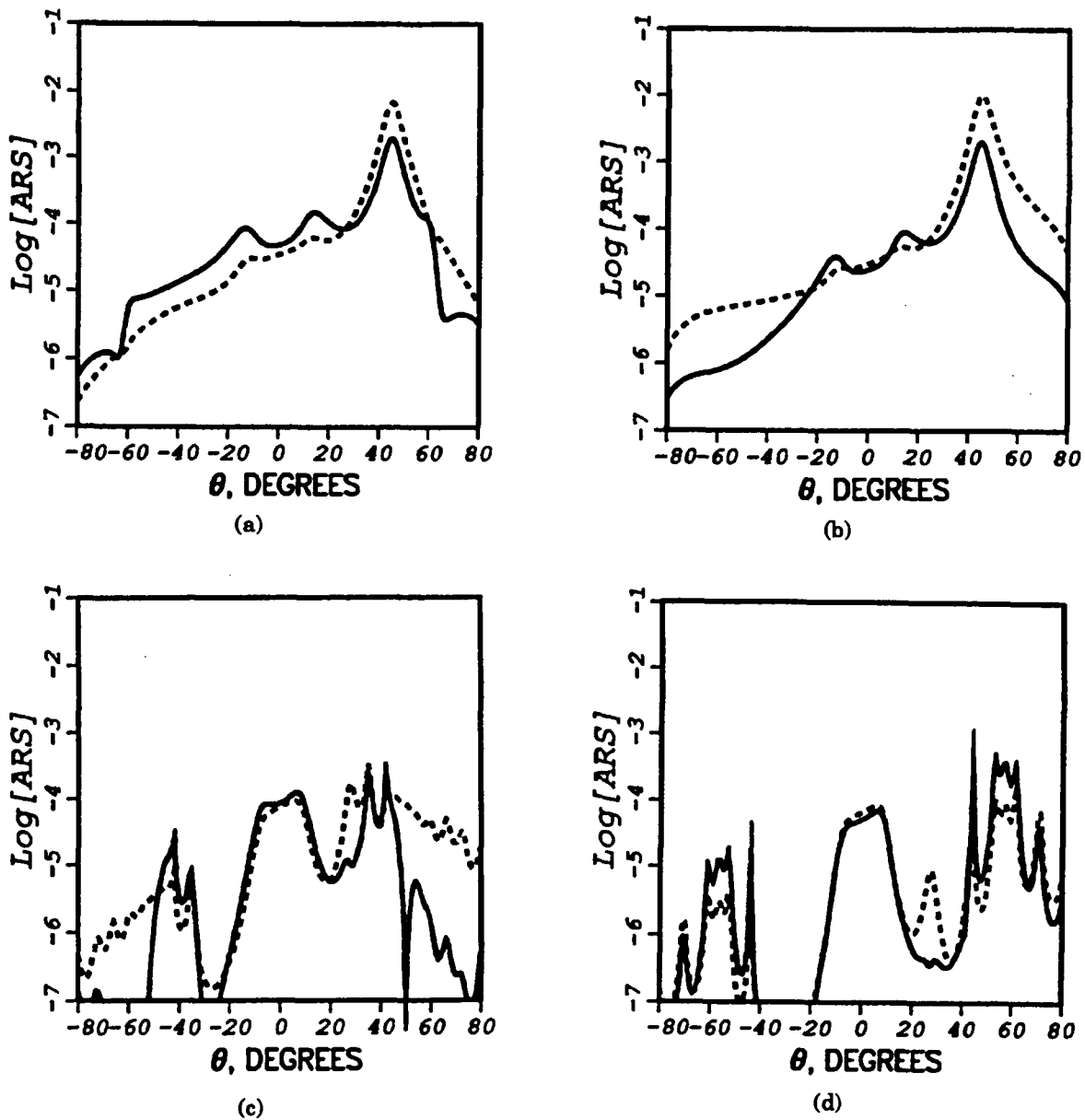


FIGURE C-1. Log[ARS] Versus Polar Scattering Angle θ . Plotted is scattering in the plane of incidence from a 28-layer multilayer stack with the incident beam of wavelength 0.65 microns incident at 45 degrees. Positive and negative θ values are for scattering azimuth angles ϕ of 0 and 180 degrees, respectively. The solid and dashed lines refer to ARS when the multilayer stack interface roughness is correlated and uncorrelated, respectively. Reflection scattering is shown in (a) and (b), and transmission scattering is shown in (c) and (d). The incident and scattered polarization for these four plots are (a) p -POL \rightarrow p -POL, (b) s -POL \rightarrow s -POL, (c) p -POL \rightarrow p -POL, and (d) s -POL \rightarrow s -POL.

Appendix D

INPUT DATA AND OUTPUT RESULTS FOR REFLECTION AND TRANSMISSION ARS FROM AN UNCOATED SURFACE AND TOTAL INTERNAL REFLECTION OF THE INCIDENT BEAM

OUTPUT DATA FILE:

SIGMA = 00.00 LAMBDA = 0.633
 THETA0 = 35.00 PHI0 = 0.00

P ⇒ p-POL scatt. S ⇒ s-POL scatt.

INPUT DATA FILE:

-80.,80.,20.
 35.0,0.633,0.0,0
 .0005,2.0,.00049,0.2
 (1.0,0.0),0.0
 (4.41,0.0),0.0

	THETA THETA	RP1 RS1	RP2 RS2	TP1 TP2	TS1 TS2
P	-80.00	0.1431E-08	0.1431E-08	0.3313E-07	0.3313E-07
S	-80.00	0.7522E-36	0.7522E-36	0.9796E-36	0.9796E-36
P	-60.00	0.1473E-07	0.1473E-07	0.1589E-06	0.1589E-06
S	-60.00	0.8622E-35	0.8622E-35	0.8856E-35	0.8856E-35
P	-40.00	0.5331E-07	0.5331E-07	0.4229E-06	0.4229E-06
S	-40.00	0.5985E-34	0.5985E-34	0.3490E-34	0.3490E-34
P	-20.00	0.2433E-05	0.2433E-05	0.1095E-05	0.1095E-05
S	-20.00	0.4018E-33	0.4018E-33	0.1161E-33	0.1161E-33
P	0.00	0.2470E-04	0.2470E-04	0.2667E-05	0.2667E-05
S	0.00	0.0000E+00	0.0000E+00	0.0000E+00	0.0000E+00
P	20.00	0.8294E-04	0.8294E-04	0.5604E-05	0.5604E-05
S	20.00	0.0000E+00	0.0000E+00	0.0000E+00	0.0000E+00
P	40.00	0.2282E-02	0.2282E-02	0.9586E-05	0.9586E-05
S	40.00	0.0000E+00	0.0000E+00	0.0000E+00	0.0000E+00
P	60.00	0.9161E-04	0.9161E-04	0.1403E-04	0.1403E-04
S	60.00	0.0000E+00	0.0000E+00	0.0000E+00	0.0000E+00

SIGMA = 90.00 LAMBDA = 0.633
 THETA0 = 35.00 PHI0 = 0.00

	THETA THETA	RP1 RS1	RP2 RS2	TP1 TP2	TS1 TS2
P	-80.00	0.1300E-35	0.1300E-35	0.4130E-35	0.4130E-35
S	-80.00	0.1119E-07	0.1119E-07	0.1458E-07	0.1458E-07
P	-60.00	0.1442E-34	0.1442E-34	0.2369E-34	0.2369E-34
S	-60.00	0.1283E-06	0.1283E-06	0.1318E-06	0.1318E-06
P	-40.00	0.8332E-34	0.8332E-34	0.8441E-34	0.8441E-34
S	-40.00	0.8908E-06	0.8908E-06	0.5194E-06	0.5194E-06
P	-20.00	0.7874E-33	0.7874E-33	0.2943E-33	0.2943E-33
S	-20.00	0.5980E-05	0.5980E-05	0.1728E-05	0.1728E-05
P	0.00	0.7175E-33	0.7175E-33	0.7748E-34	0.7748E-34
S	0.00	0.4272E-04	0.4272E-04	0.4612E-05	0.4612E-05
P	20.00	0.2410E-32	0.2410E-32	0.1628E-33	0.1628E-33
S	20.00	0.2038E-03	0.2038E-03	0.8843E-05	0.8843E-05
P	40.00	0.6630E-31	0.6630E-31	0.2785E-33	0.2785E-33
S	40.00	0.2301E-02	0.2301E-02	0.1177E-04	0.1177E-04
P	60.00	0.2662E-32	0.2662E-32	0.4077E-33	0.4077E-33
S	60.00	0.9495E-04	0.9495E-04	0.1164E-04	0.1164E-04

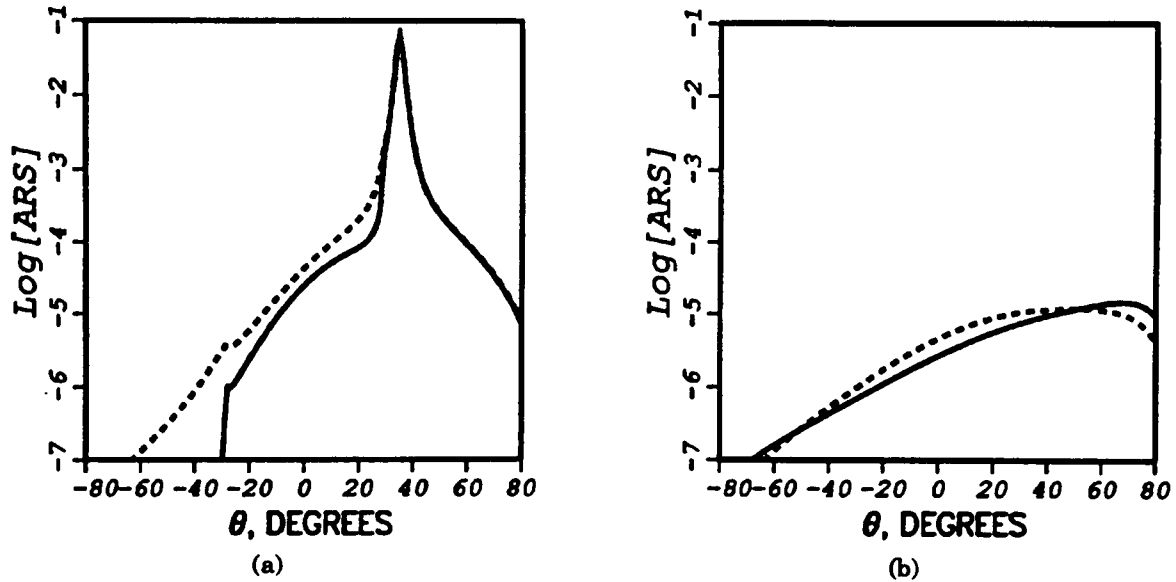


FIGURE D-1. Log[ARS] Versus Polar Scattering Angle θ . Plotted is scattering in the plane of incidence from a bare surface ($L = 0$) with the incident beam of wavelength 0.633 microns incident at 35 degrees. This angle of incidence is beyond the critical angle for specular transmission. Positive and negative θ values are for scattering azimuth angles ϕ of 0 and 180 degrees, respectively. The solid and dashed lines refer to ARS when the incident and scattered polarization are $p-POL \rightarrow p-POL$ and $s-POL \rightarrow s-POL$, respectively. Reflection scattering is shown in (a), and transmission scattering is shown in (b). Since there is only one interface, the correlated and uncorrelated cases give identical results.

Appendix E

INPUT DATA AND OUTPUT RESULTS FOR OUT-OF-PLANE ARS
FROM A FIVE-LAYER STACK UPON A METALLIC SUBSTRATE

OUTPUT DATA FILE:

SIGMA = 0.00 LAMBDA = 0.633
THETA0 = 60.00 PHI0 = 35.00

P ⇒ p-POL scatt. S ⇒ s-POL scatt.

INPUT DATA FILE:

-80.,80.,20.
60.,0.633,35.0,5
.0005,2.0.,.00049,0.2
(-16.0,0.5),0.0
(4.41,0.0),0.4
(2.25,0.0),0.6
(4.41,0.0),0.4
(2.25,0.0),0.6
(4.41,0.0),0.7
(1.0,0.0),0.0

	THETA THETA	RP1 RS1	RP2 RS2	TP1 TP2	TS1 TS2
P	-80.00	0.2290E-06	0.1626E-05	0.0000E+00	0.0000E+00
S	-80.00	0.3360E-07	0.0086E-06	0.0000E+00	0.0000E+00
P	-60.00	0.6770E-05	0.1013E-04	0.0000E+00	0.0000E+00
S	-60.00	0.3337E-06	0.1760E-05	0.0000E+00	0.0000E+00
P	-40.00	0.4994E-06	0.8653E-05	0.0000E+00	0.0000E+00
S	-40.00	0.2639E-08	0.1664E-05	0.0000E+00	0.0000E+00
P	-20.00	0.6324E-05	0.6358E-04	0.0000E+00	0.0000E+00
S	-20.00	0.1478E-05	0.2828E-04	0.0000E+00	0.0000E+00
P	0.00	0.3432E-04	0.5208E-04	0.0000E+00	0.0000E+00
S	0.00	0.1683E-04	0.2553E-04	0.0000E+00	0.0000E+00
P	20.00	0.6859E-05	0.1441E-03	0.0000E+00	0.0000E+00
S	20.00	0.4203E-05	0.8042E-04	0.0000E+00	0.0000E+00
P	40.00	0.1018E-04	0.4903E-04	0.0000E+00	0.0000E+00
S	40.00	0.1887E-07	0.1190E-04	0.0000E+00	0.0000E+00
P	60.00	0.5383E-06	0.9180E-04	0.0000E+00	0.0000E+00
S	60.00	0.4297E-05	0.2266E-04	0.0000E+00	0.0000E+00

SIGMA = 90.00 LAMBDA = 0.633
THETA0 = 60.00 PHI0 = 35.00

	THETA THETA	RP1 RS1	RP2 RS2	TP1 TP2	TS1 TS2
P	-80.00	0.4551E-07	0.2326E-06	0.0000E+00	0.0000E+00
S	-80.00	0.1600E-07	0.1153E-06	0.0000E+00	0.0000E+00
P	-60.00	0.3337E-06	0.1760E-05	0.0000E+00	0.0000E+00
S	-60.00	0.1812E-06	0.1845E-05	0.0000E+00	0.0000E+00
P	-40.00	0.1603E-08	0.1610E-05	0.0000E+00	0.0000E+00
S	-40.00	0.5651E-07	0.1780E-05	0.0000E+00	0.0000E+00
P	-20.00	0.1200E-06	0.1478E-04	0.0000E+00	0.0000E+00
S	-20.00	0.5996E-06	0.3106E-04	0.0000E+00	0.0000E+00
P	0.00	0.4013E-05	0.1217E-04	0.0000E+00	0.0000E+00
S	0.00	0.8184E-05	0.2482E-04	0.0000E+00	0.0000E+00
P	20.00	0.3412E-06	0.4202E-04	0.0000E+00	0.0000E+00
S	20.00	0.1705E-05	0.8831E-04	0.0000E+00	0.0000E+00
P	40.00	0.1146E-07	0.1151E-04	0.0000E+00	0.0000E+00
S	40.00	0.4041E-06	0.1273E-04	0.0000E+00	0.0000E+00
P	60.00	0.4297E-05	0.2266E-04	0.0000E+00	0.0000E+00
S	60.00	0.2333E-05	0.2375E-04	0.0000E+00	0.0000E+00

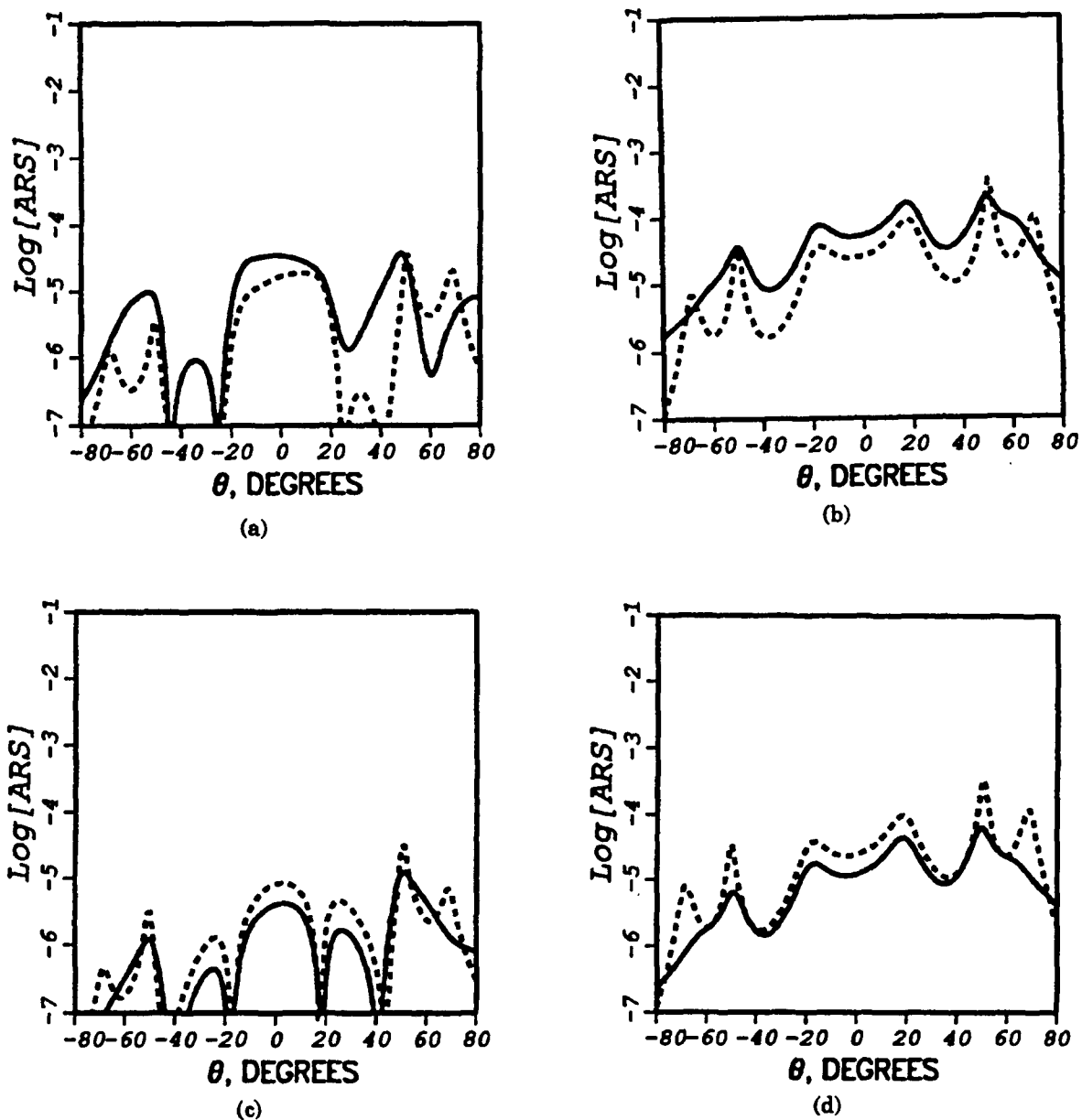


FIGURE E-1. Log[ARS] Versus Polar Scattering Angle θ . Plotted is out-of-plane scattering from a five-layer multilayer stack with the incident beam of wavelength 0.633 microns incident at 60 degrees. Positive and negative θ values are for scattering azimuth angles ϕ of 35 and 215 degrees, respectively. ARS from a correlated multilayer stack is shown in (a) where the solid and dashed lines are for incident and scattered polarizations $p\text{-POL} \rightarrow p\text{-POL}$ and $p\text{-POL} \rightarrow s\text{-POL}$, respectively. ARS from an uncorrelated multilayer stack is shown in (b) where the solid and dashed lines are for incident and scattered polarizations $p\text{-POL} \rightarrow p\text{-POL}$ and $p\text{-POL} \rightarrow s\text{-POL}$, respectively. ARS from a correlated multilayer stack is shown in (c) where the solid and dashed lines are for incident and scattered polarizations $s\text{-POL} \rightarrow p\text{-POL}$ and $s\text{-POL} \rightarrow s\text{-POL}$, respectively. Finally, ARS from an uncorrelated multilayer stack is shown in (d) where the solid and dashed lines are for incident and scattered polarizations $s\text{-POL} \rightarrow p\text{-POL}$ and $s\text{-POL} \rightarrow s\text{-POL}$, respectively.

Appendix F

INPUT DATA AND OUTPUT RESULTS FOR ARS FROM A SEMI-OPAQUE THIN METALLIC FILM INCLUDING SURFACE PLASMA RESONANCE

OUTPUT DATA FILE:

SIGMA = 0.00 LAMBDA = 0.633
 THETA0 = 29.60 PHI0 = 0.00

P ⇒ p-POL scatt. S ⇒ s-POL scatt.

INPUT DATA FILE:

-80.,80.,20.
 29.6,0.633,0.0,1
 .0005,2.0.,00049,0.2
 (1.0,0.0),0.0
 (-16.0,0.5),0.025
 (4.41,0.0),0.0

	THETA THETA	RP1 RS1	RP2 RS2	TP1 TP2	TS1 TS2
P	-80.00	0.9282E-07	0.4515E-06	0.7616E-05	0.1086E-04
S	-80.00	0.9677E-37	0.7410E-35	0.2524E-34	0.5526E-34
P	-60.00	0.1013E-05	0.4664E-05	0.2858E-04	0.4199E-04
S	-60.00	0.5628E-36	0.1005E-33	0.3041E-33	0.6638E-33
P	-40.00	0.1272E-04	0.4540E-04	0.5558E-04	0.8714E-04
S	-40.00	0.1164E-35	0.1076E-32	0.1438E-32	0.3125E-32
P	-20.00	0.2593E-04	0.1451E-03	0.9204E-04	0.1620E-03
S	-20.00	0.6472E-33	0.1907E-31	0.5064E-32	0.1096E-31
P	0.00	0.5561E-04	0.1221E-02	0.1103E-03	0.2383E-03
S	0.00	0.0000E+00	0.0000E+00	0.0000E+00	0.0000E+00
P	20.00	0.6053E-04	0.5371E-02	0.7901E-04	0.2540E-03
S	20.00	0.0000E+00	0.0000E+00	0.0000E+00	0.0000E+00
P	40.00	0.3037E-04	0.6166E-02	0.3026E-04	0.2375E-03
S	40.00	0.0000E+00	0.0000E+00	0.0000E+00	0.0000E+00
P	60.00	0.1903E-04	0.1190E-02	0.4425E-05	0.5173E-03
S	60.00	0.0000E+00	0.0000E+00	0.0000E+00	0.0000E+00

SIGMA = 90.00 LAMBDA = 0.633
 THETA0 = 29.60 PHI0 = 0.00

	THETA THETA	RP1 RS1	RP2 RS2	TP1 TP2	TS1 TS2
P	-80.00	0.9427E-35	0.2177E-34	0.1645E-33	0.3375E-33
S	-80.00	0.1480E-07	0.2585E-07	0.3452E-08	0.4845E-07
P	-60.00	0.9127E-34	0.2153E-33	0.6079E-33	0.1315E-32
S	-60.00	0.1838E-06	0.3349E-06	0.4370E-07	0.5827E-06
P	-40.00	0.7838E-33	0.1847E-32	0.1138E-32	0.2777E-32
S	-40.00	0.1611E-05	0.3236E-05	0.2219E-06	0.2748E-05
P	-20.00	0.5873E-32	0.7613E-32	0.1738E-32	0.5331E-32
S	-20.00	0.2058E-04	0.4852E-04	0.8282E-06	0.9656E-05
P	0.00	0.1616E-32	0.3548E-31	0.3205E-32	0.6925E-32
S	0.00	0.1545E-03	0.3602E-03	0.2143E-05	0.2442E-04
P	20.00	0.1759E-32	0.1561E-30	0.2296E-32	0.7381E-32
S	20.00	0.6590E-03	0.1554E-02	0.3543E-05	0.4131E-04
P	40.00	0.8825E-33	0.1791E-30	0.8791E-33	0.6900E-32
S	40.00	0.5025E-03	0.1009E-02	0.4206E-05	0.5210E-04
P	60.00	0.5530E-33	0.3456E-31	0.1286E-33	0.1503E-31
S	60.00	0.7567E-04	0.1379E-03	0.7709E-05	0.1028E-03

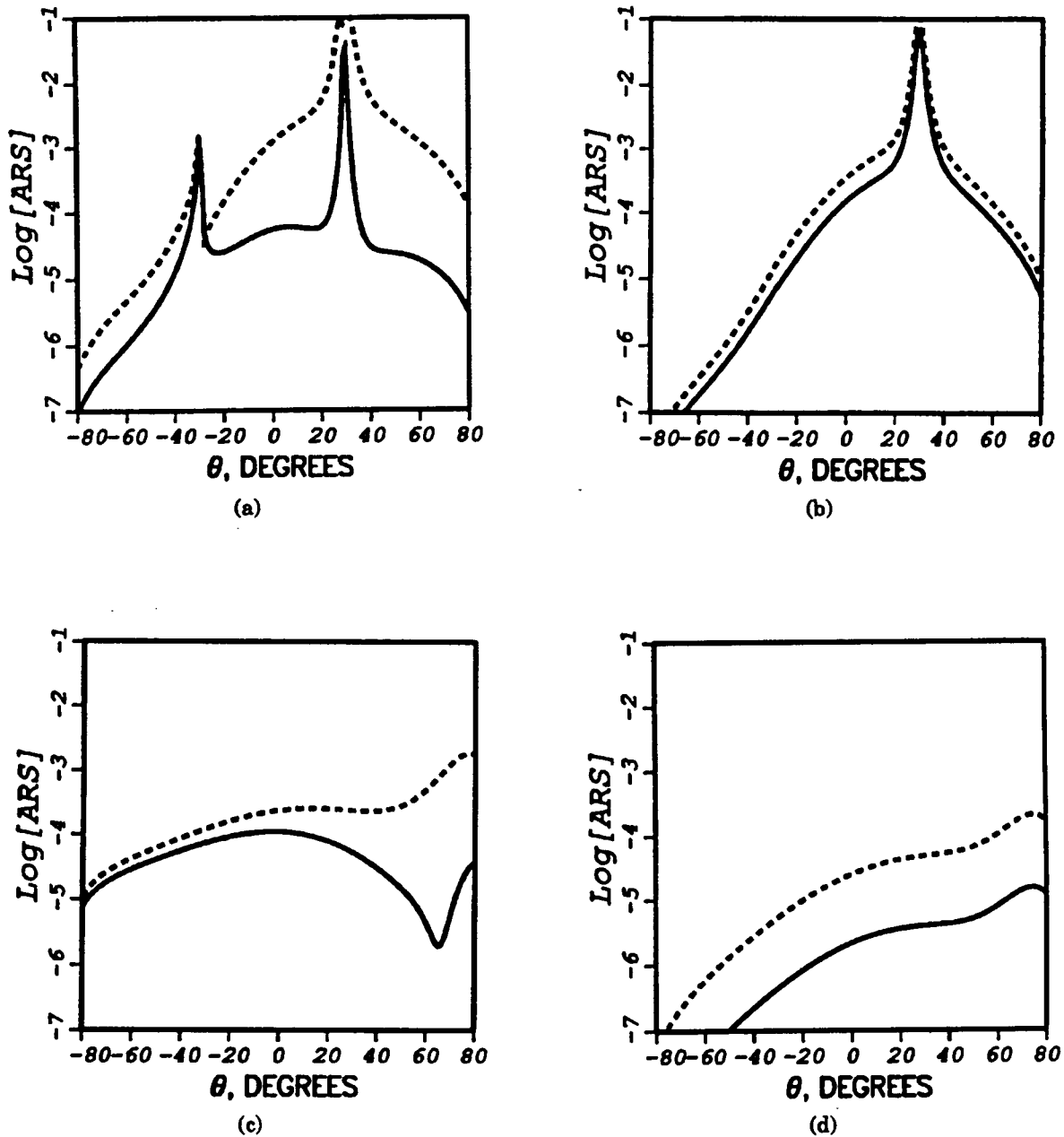


FIGURE F-1. $\text{Log}[\text{ARS}]$ Versus Polar Scattering Angle θ . Plotted is scattering in the plane of incidence for a single-layer case ($L = 1$) with the incident beam of wavelength 0.633 microns incident at 29.6 degrees. Positive and negative θ values are for scattering azimuth angles ϕ of 0 and 180 degrees, respectively. The solid and dashed lines refer to ARS when the multilayer stack interface roughness is correlated and uncorrelated, respectively. Reflection scattering is shown in (a) and (b), and transmission scattering is shown in (c) and (d). The incident and scattered polarization for these four plots are (a) $p\text{-POL} \rightarrow p\text{-POL}$, (b) $s\text{-POL} \rightarrow s\text{-POL}$, (c) $p\text{-POL} \rightarrow p\text{-POL}$, and (d) $s\text{-POL} \rightarrow s\text{-POL}$.

INITIAL DISTRIBUTION

- 1 Commander in Chief, U. S. Pacific Fleet, Pearl Harbor (Code 325)
- 1 Commander, Third Fleet
- 1 Commander, Seventh Fleet
- 1 Naval War College, Newport (Technical Library)
- 1 Air Force Intelligence Agency, Bolling Air Force Base (AFIA/INT, MAJ R. Esaw)
- 2 Defense Technical Information Center, Alexandria
- 1 Center for Naval Analyses, Alexandria, VA (Technical Library)
- 2 Optical Coating Laboratory, Incorporated, Santa Rosa, CA
 - J. Apfel (1)
 - J. Rancourt (1)